

# Modeling Storm Surge in a Small Tidal Two-inlet System

Matthew Reffitt<sup>1</sup>, Mara M. Orescanin<sup>2</sup>, Chris Massey<sup>3</sup>, Britt Raubenheimer<sup>4</sup>,  
Robert E. Jensen<sup>5</sup>, and Steve Elgar<sup>6</sup>

<sup>1</sup>Naval Postgraduate School, Department of Oceanography, Monterey, CA, USA

<sup>2</sup>Naval Postgraduate School, Department of Oceanography, Monterey, CA, USA

<sup>3</sup>US Army, Engineering Research and Development Center, Coastal Hydraulics Laboratory,  
Vicksburg, MS, USA

<sup>4</sup>Woods Hole Oceanographic Institution, Woods Hole, MA, USA

<sup>5</sup>US Army, Engineering Research and Development Center, Coastal Hydraulics Laboratory,  
Vicksburg, MS, USA

<sup>6</sup>Woods Hole Oceanographic Institution, Woods Hole, MA, USA

## ABSTRACT

Model simulations using a depth-averaged ocean circulation model (ADCIRC) two-way coupled with a wave model (STWAVE) through the Coastal Storm Modeling System Coupling Framework (CSTORM-MS) are compared with observations made in the shallow, two-inlet tidal Katama Bay system on the Atlantic coast of Martha's Vineyard, Massachusetts during Hurricane Irene. The CSTORM-MS framework integrates high-resolution bathymetric grids of this system with the North Atlantic Coast Comprehensive Study (NACCS) performed by the United States Army Corps of Engineers. The effects of bathymetric resolution and wave-flow coupling on the accuracy of modeled storm surge were investigated by comparing observations with the high bathymetric resolution, coupled model (CSTORM), a high-resolution uncoupled ADCIRC model, and a low bathymetric resolution, coupled model (NACCS). During the peak storm surge period, the coupled model using high-spatial resolution bathymetry reduced error in the study area by over 30 percent compared with the lower-resolution NACCS model, and by 16 percent compared with the high-resolution, uncoupled ADCIRC model. In addition, the high-resolution models indicate alongshore flows with magnitudes over 2.0 m/s along the southern coast of Martha's Vineyard, and a net northward circulation through Katama Bay and Edgartown Channel, which are not apparent in the lower-resolution simulations. Contrary to prior research suggesting small, if any setup in the Katama Bay system from wave forcing, in the extreme wave forcing event discussed here, the northward flux through Katama Inlet on the south side of the bay does not exit completely through Edgartown Channel on the north side of Katama Bay.

37 Thus, the drainage path is not adequate to prevent increased water elevation in the bay, resulting  
38 in a setup within Katama Bay during the peak surge event, highlighting the need for adequate  
39 model resolution for local storm surge predictions.

40  
41

## 42 **1.INTRODUCTION**

### 43 **1.1 BACKGROUND**

44 Storm surge, or the increase in water level associated with a meteorological event, often  
45 accounts for a significant percentage of the property damage caused by hurricanes (Neumann et  
46 al. 2015). In addition, coastal flooding associated with storm surge can create a hazard to  
47 residents that often is a major contributor to high death tolls (Blake et al. 2007). To provide  
48 adequate warning to prevent the loss of life and property, storm surge must be predicted  
49 accurately. However, storm surge in spatially small systems with complex bathymetry, such as  
50 tidal inlets, can be difficult to predict with regional-scale storm-surge forecast modeling systems  
51 that necessitate coarse spatial resolution (Yin et al. 2016). For example, storm surge in inland  
52 areas of the US Gulf Coast was not predicted accurately with low-resolution models during  
53 Hurricane Ike (Kerr et al. 2013), nor was storm surge predicted accurately for barrier island  
54 systems along the US East Coast (Lawler et al., 2016; Bennett et al., 2018).

55 Coupling high-resolution storm-surge models with nearshore wave models is an active  
56 research field (Dietrich et al. 2012; Orton et al. 2012; Sun et al. 2013; Mao and Xia, 2018; Kang  
57 and Xia, 2020) motivated by observations of wave effects on water levels in back lagoons and  
58 currents within tidal inlets (Bertin, et al. 2009; Malhadas et al., 2009; Dodet et al. 2013;  
59 Orescanin et al. 2014). There are several examples of such modeling systems, including the  
60 coupling of the unstructured version of the Simulating Waves Nearshore (SWAN) and the  
61 Advanced Circulation (ADCIRC) models (Dietrich et al. 2012), coupling of Delft3D and SWAN  
62 (Bennett et al. 2018), the Coupled-Ocean-Atmosphere-Wave-Sediment Transport (COAWST)  
63 model, (Kumar et al. 2012), and FVCOM/SWAVE (Chen et al. 2013). Neglecting small-scale  
64 bathymetric features, such as tidal inlets or shoals, and the associated hydrodynamics, can lead to  
65 under prediction of storm surge relative to simulations that include high-resolution bathymetry  
66 and small-scale processes (Orton et al. 2012; Sun et al. 2013).

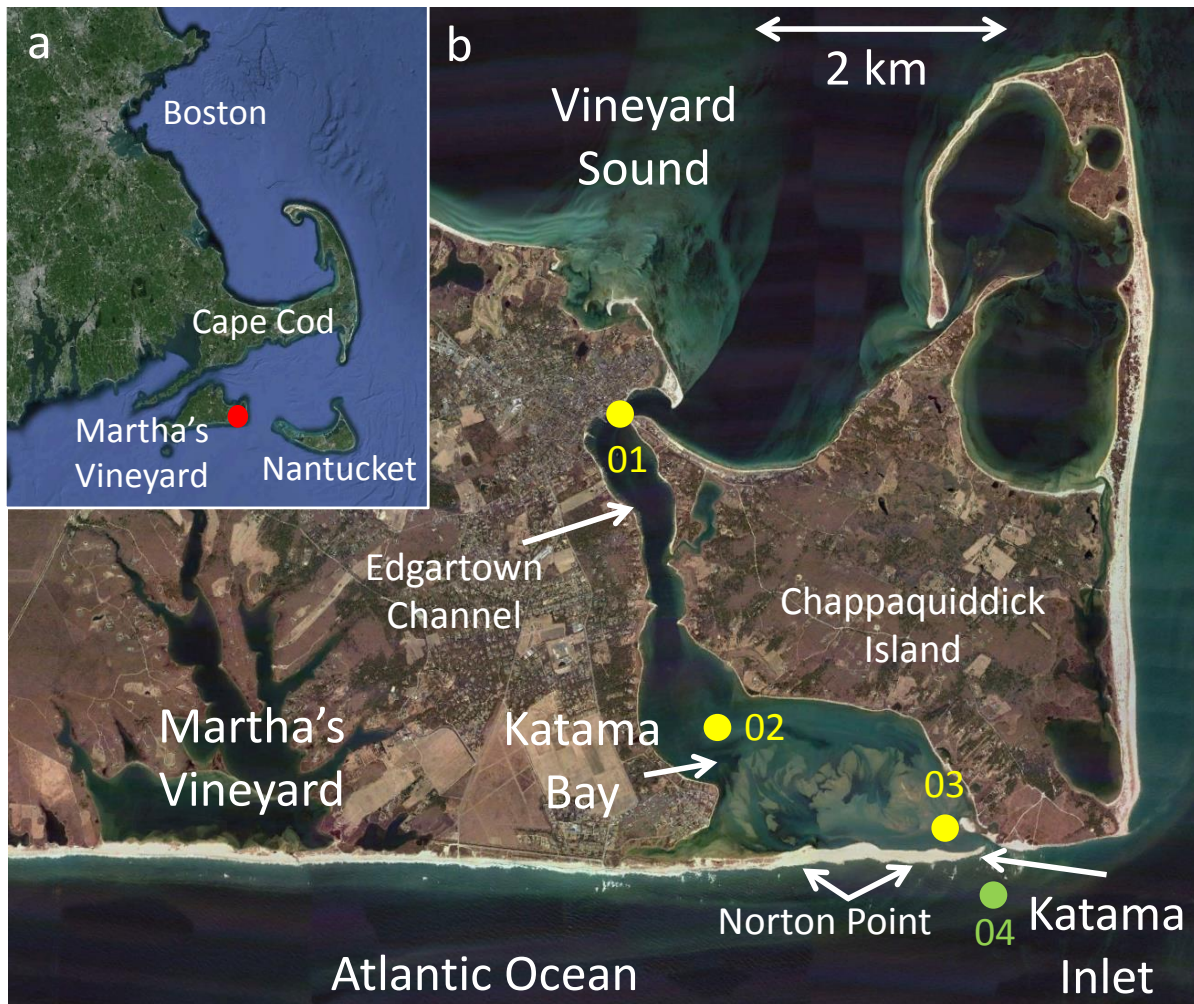
67           The Steady-State Spectral Wave Model (STWAVE) accounts for both wave diffraction  
68 and reflection (Gonçalves et al. 2015), which may be important near the complex bathymetry of  
69 tidal inlet systems where observations show large spatial gradients of currents, waves, and  
70 bathymetry. Using the Coastal Storm Modeling System Coupling Framework (CSTORM-MS)  
71 (Massey et al. 2011), STWAVE and ADCIRC coupled modeling of storm surge is skillful on  
72 large spatial scales (Bryant and Jensen 2017). Less research has been conducted at the higher  
73 resolutions needed to resolve most inlet and small bay systems that are common along barrier  
74 island coastlines. Model domain sizes that are not sufficiently large underestimate storm surge  
75 (Blain et al. 1994), therefore nested model domains are an option to increase resolution in areas  
76 of interest, while minimizing computational cost.

## 77 **1.2 STUDY PARAMETERS**

78           The focus here is the Katama Inlet system, Martha’s Vineyard, Massachusetts (Figure 1),  
79 during Hurricane Irene. Pressure sensors were deployed in the Bay from Katama Inlet in the  
80 south to Edgartown Channel in the north in early August, 2011, and remained in place until after  
81 Hurricane Irene (Figure 1, and Orescanin et al. 2014). The observations are used here to  
82 examine the skill of coupled wave and circulation models with different spatial resolutions.

83

84

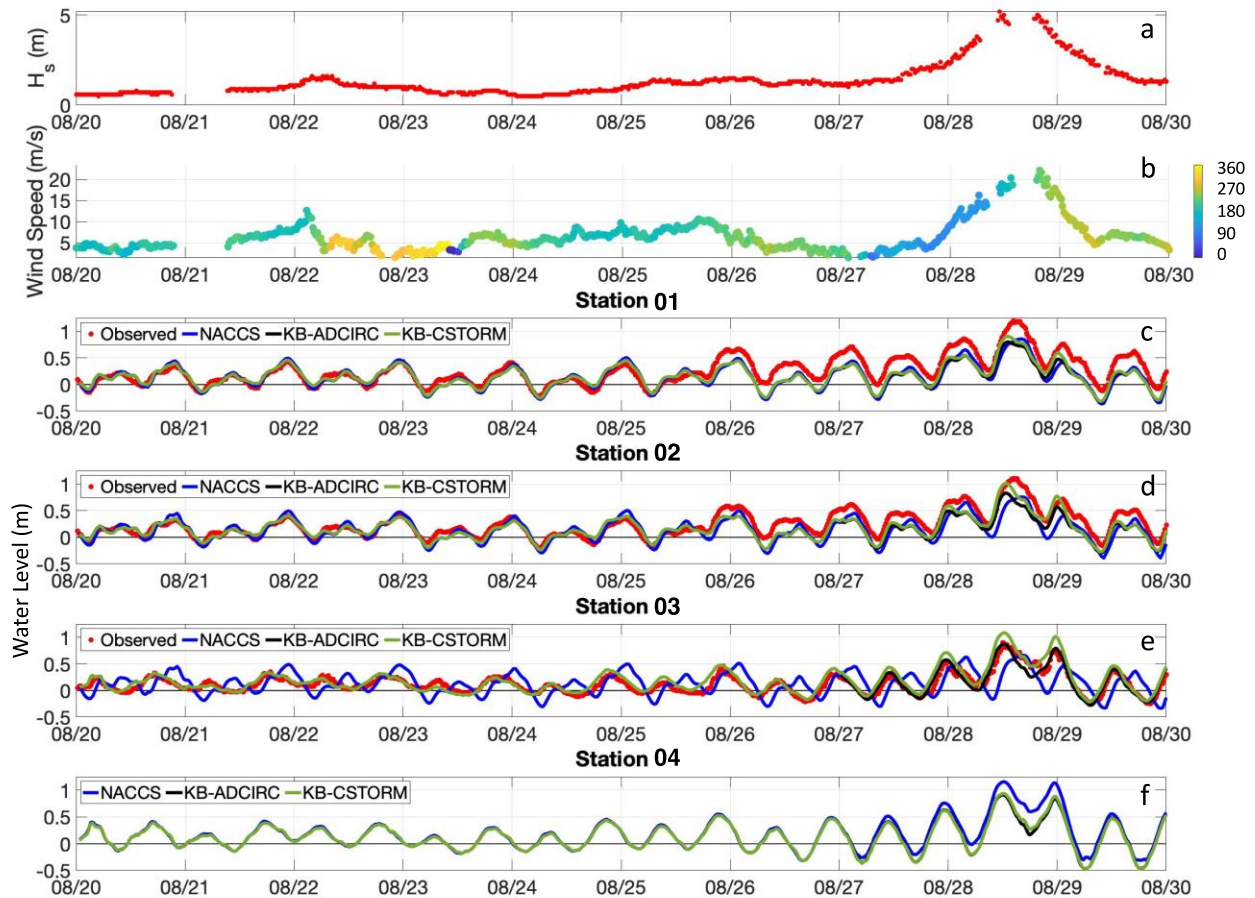


85

86 **Figure 1:** Location of (a) Martha's Vineyard, MA, with the Katama system inside the red  
 87 circle, and (b) the south-eastern part of Martha's Vineyard, showing Katama Bay, with  
 88 Edgartown Channel to the north and Katama Inlet to the south. The yellow circles are  
 89 sensor locations and the green circle (04) is located on the ebb shoal where model results  
 90 are compared with each other.

91 Irene (Atlantic storm number 09) passed approximately 550 km to the west on 28 August,  
 92 2011. Significant wave heights measured at the closest offshore NOAA buoy (number 44097)  
 93 reached a peak of 14.7 m at 12:38 EDT on August 28, much higher than the typical non-storm  
 94 value of 1.0 m. Martha's Vineyard Coastal Observatory (MVCO) recorded significant wave  
 95 heights over 5 m in 12-m water depth (Figure 2a). Maximum sustained winds at the NOAA  
 96 buoy at Buzzards Bay located 55 km to the west of the research area and at MVCO (Figure 2b)  
 97 at the time of the closest point of approach were approximately 25 m/s. Storm surge associated  
 98 with Irene propagated northward through the research area, and was 0.7 m at the southernmost

99 observation sensor in Katama Bay (Station 03 in Figure 1, red time series in Figure 2e) on  
100 August 28 at 14:45 EDT.



101  
102 **Figure 2:** Time series of waves, wind speed and direction, and water level for the Katama Bay  
103 system: a) Significant wave height ( $H_s$ ) and b) wind speed (colored by direction, scale on the  
104 right) for MVCO (12 m depth), and water-surface elevation for c) Station 01, d) Station 02, e)  
105 Station 03, and f) Station 04 versus time during Hurricane Irene, which had maximum impact in  
106 this area mid-day on 08/28. The curves are for observations (red), NACCS (blue), KB-ADCIRC  
107 (black), and KB-CSTORM (green). Observations were not obtained at Station 04.

108

109 Katama Bay and the surrounding Atlantic Ocean (including Wasque Shoals, south of  
110 Katama Inlet) is an area of complex bathymetry that includes the migrating Katama Inlet that,  
111 when open, connects the southern part of the bay with the Atlantic Ocean (Figure 1). Katama  
112 Inlet last opened during a nor'easter storm in 2007, and slowly migrated 1.5 km to the east until  
113 it closed in 2015, producing complicated, evolving ebb and flood shoals. These shoals and

114 Norton Point are comprised of medium sand. Katama Bay is connected to Vineyard Sound in the  
115 north by the continuously open Edgartown Channel (Figure 1). Thus, when Katama Inlet is open,  
116 this site is a double inlet system. The M2 tide at Edgartown Channel in Vineyard Sound is  
117 approximately three hours out of phase (delayed) with the Atlantic M2 tides at Katama  
118 Inlet. This phase difference results in strong tidal flows in the inlets and the bay. However,  
119 under normal conditions sub-tidal changes in the bay sea level are small because water can flow  
120 out of the inlets (Orescanin et al., 2014). In addition, there is no significant freshwater input to  
121 the system that would distort the tidally driven flows.

122         The complex bathymetry covers a relatively small area, and thus is an ideal location to  
123 study the effects of spatial resolution on models for storm surge. Previous modeling in this area  
124 focused on wave-current interaction (Hopkins et al. 2016), sediment transport processes  
125 (Hopkins et al. 2017), and the effect of temporally varying inlet geometry on bay circulation  
126 (Orescanin et al. 2016). Numerical results suggest that high-spatial-resolution bathymetry, both  
127 within Katama Bay and in the Atlantic Ocean offshore of Katama Inlet, combined with accurate  
128 wave models are critical to simulate the hydrodynamics of the system.

129         Here, the importance of spatial resolution and wave forcing to simulations of storm surge  
130 through small coastal bays and inlets is investigated. Specifically, STWAVE and ADCIRC are  
131 dynamically two-way coupled using the CSTORM coupler, and the peak storm surge and flow  
132 predictions are compared with the predictions of uncoupled or lower-resolution modeling  
133 systems. Large domain ADCIRC meshes and STWAVE grids created by the United States Army  
134 Corps of Engineers for the North Atlantic Coast Comprehensive Study (NACCS) (Cialone et al.  
135 2015; Cialone et al., 2017) are utilized and merged with higher resolution grids.

136

137

## 138 **2 CSTORM NUMERICAL MODELS**

139 The Coastal Storm Modeling System (CSTORM-MS) is a system of numerical models used to  
140 simulate coastal storm waves and water levels, as well as a comprehensive methodology of how  
141 those models are applied to provide accurate inputs for assessing risk to coastal communities.

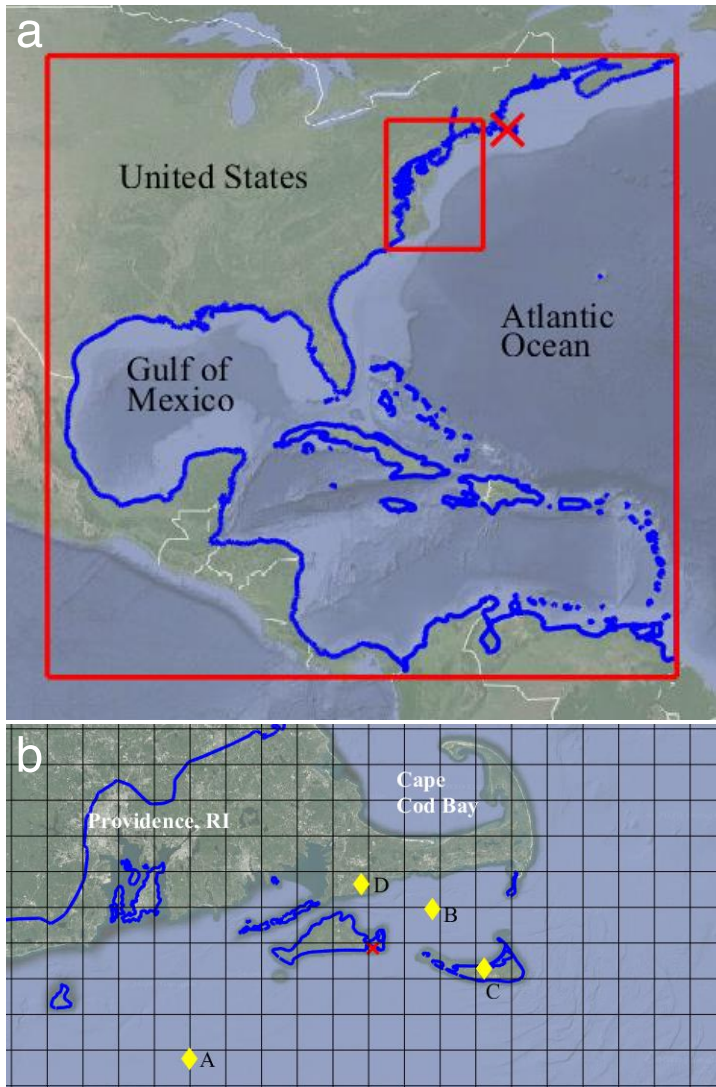
142 The CSTORM-MS makes use of nonlinear physics-based models with higher-order-accurate

143 numerical discretization methods and resolutions. The numerical models used within the  
144 CSTORM modeling system for the NACCS consisted of the deep water Wave Model (WAM)  
145 for producing offshore wave boundary conditions for use with the nearshore STWAVE model.  
146 ADCIRC model was used to simulate two-dimensional depth-integrated surge and circulation  
147 responses to the storm conditions. The STWAVE model was used to provide the nearshore wave  
148 conditions, including local wind-generated waves. The CSTORM coupling framework (Massey  
149 et al. 2011) was used to tightly two-way couple the ADCIRC and STWAVE models to allow for  
150 dynamic interactions between the surge, circulation, and waves, resulting in improved modeling  
151 results.

152

## 153 **2.1 WIND AND PRESSURE FIELDS**

154 The wind and pressure fields used for the Hurricane Irene simulations were produced by  
155 Oceanweather, Inc. (OWI, 2015) and are the same winds and pressures used and documented as  
156 part of the NACCS (Cialone et.al 2015). Two levels of wind and pressure fields were used.  
157 (Figure 3). The first level included a larger domain covering the western Atlantic and from 99.0  
158 to 60.0 degrees west longitude and from 7.500 to 46.125 degrees north latitude using a 0.125-  
159 degree grid resolution (larger grid, Figure 3a). The second level covered an area from 78.00 to  
160 72.00 degrees west longitude and from 34.00 to 42.05 degrees north latitude using a grid  
161 resolution of 0.05 degrees (smaller grid, Figure 3). The wind and pressure field records were  
162 sampled every 15 minutes, and covered the period from 08/20/2011 0 hr UTC to 08/30/2011 0 hr  
163 UTC. The study area (red X, Figure 3a) was located in the larger wind and pressure domain with  
164 a gridded resolution of 0.125 degrees.



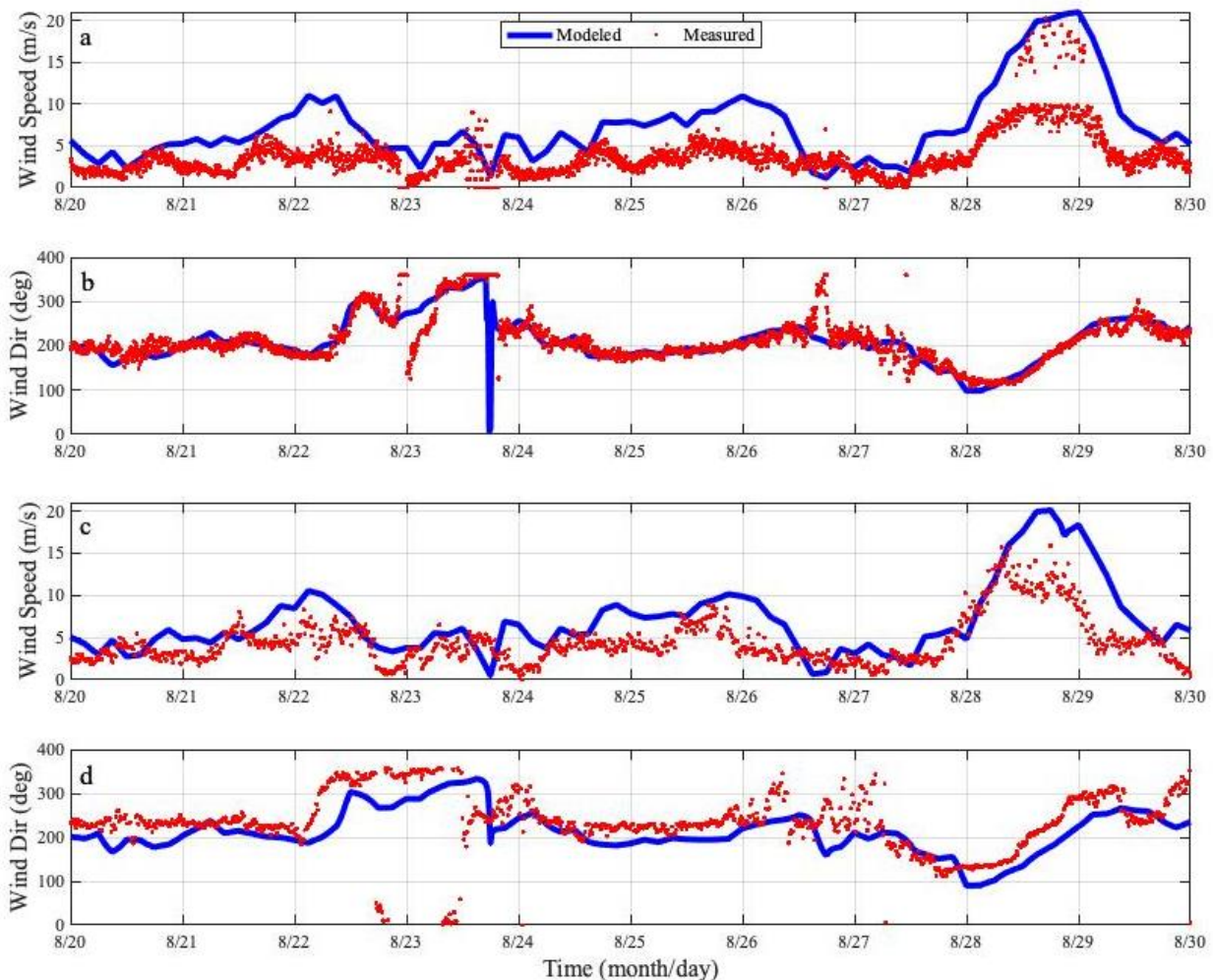
165  
 166 Figure 3: a) Map showing the outline of the ADCIRC model domain boundaries in dark blue  
 167 and the boundaries of the two wind and pressure field domains in red. A red X demarks the  
 168 study area. b) Map showing a more detailed view of the project area, with the ADCIRC model  
 169 domain boundaries in dark blue and the black gridded lines showing the grid cells for the level 1  
 170 wind and pressure fields. Winds were observed at the 4 locations marked with yellow diamonds,  
 171 with waves observed at yellow diamonds A and B. The red X demarks the study area.

172

173 Several National Data Buoy Center (NDBC) and one National Estuarine Research  
 174 Reserve System (NERRS) locations recorded wind speeds and directions during Hurricane Irene  
 175 near the study area. Of those, three representative sites were selected to compare wind speeds  
 176 and directions, and two sites were selected to compare wave statistics (yellow diamonds in  
 177 Figure 3b). The selected NDBC sites for wind comparisons are NTKM3 (“C” in Figure 3b) on



178 Nantucket Island, MA (Figure 4a,b) and Station 44020 (“B” in Figure 3b) in Nantucket Sound  
179 (Figure 5). The measured and modeled wind speeds are similar (Figures 4-5), with the modeled  
180 values for peak wind speeds slightly over-predicted by approximately 5 m/s at Station NTKM3  
181 and the Waquoit Bay Reserve NERRS (Figures 4a and 4c). The wind directions at these  
182 locations (Figures 4b, 4d, and 5f) also compare well, although there is an approximately 30-  
183 degree shift in the wind directions at the NERRS location. Considering the 0.125 degree  
184 resolution of the modeled winds, the simulated values are considered to represent the storm well  
185 in this small bay.  
186



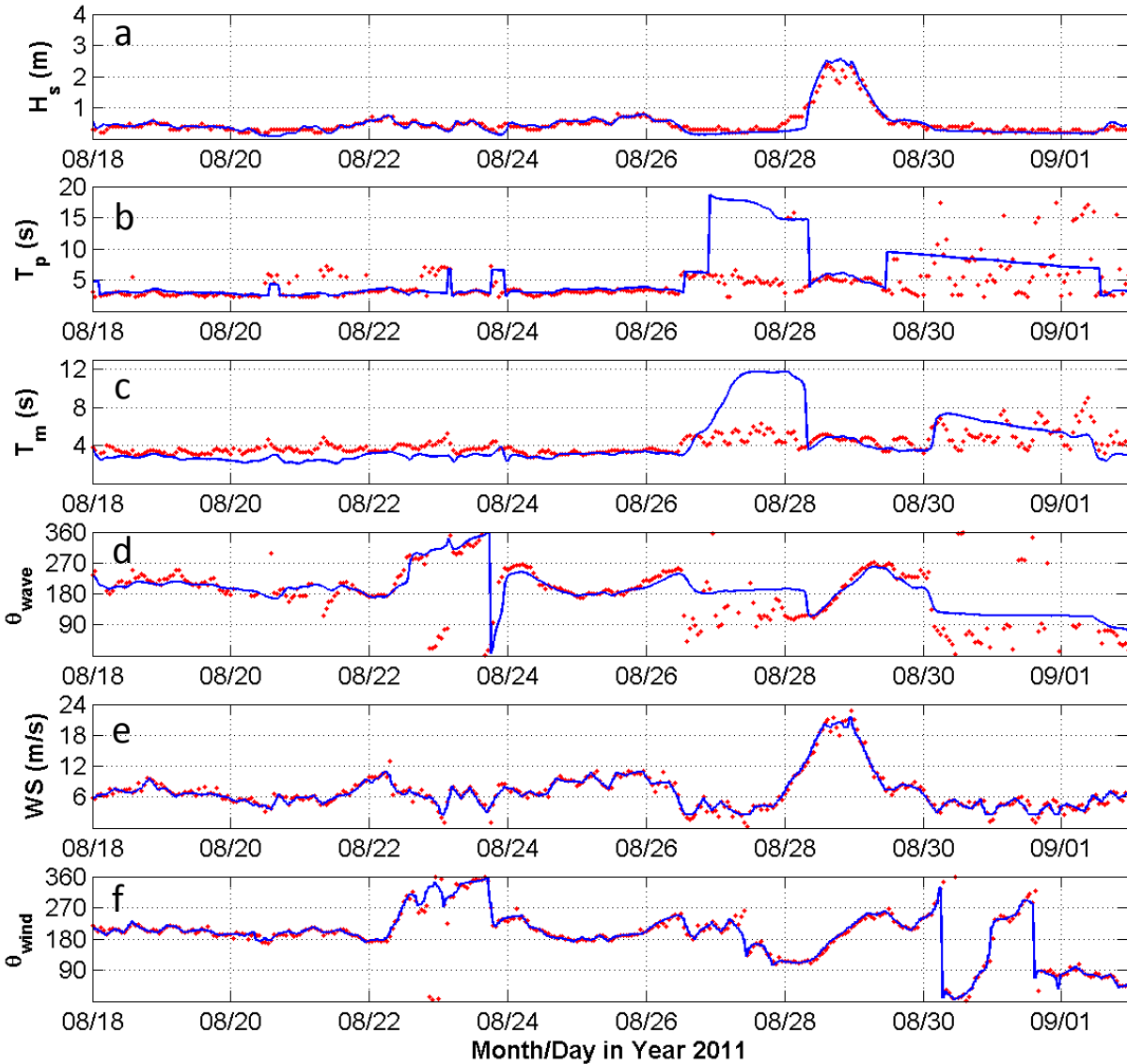
187  
188 Figure 4: Time series of wind speed and direction at (a-b) NDBC NTKM3 (Nantucket) and (c-d)  
189 NERRS Waquoit Bay Reserve. WAM model inputs used for the NACCS (blue) compared with  
190 observations (red). Locations for NTKM3 and Waquoit Bay are shown in Figure 3b (positions C  
191 and D, respectively).  
192

193        **2.2 WAM WAVE MODEL**

194    The deep-water wave model used to generate the offshore wave estimates for the NACCS and  
195    consequently for this study, is the 3rd generation wave model WAM (Komen et al., 1994).  
196    WAM is similar to other 3rd generation wave models like WaveWatch III (Tolman, 2014) or  
197    SWAN (The SWAN Team, 2017). WAM makes no a priori assumptions governing the spectral  
198    shape of the waves and the source term solution is formulated to the wave model's  
199    frequency/directional resolution. WAM was developed by a consortium of wave theoreticians  
200    and modelers over a ten-year period and is used by the European Center for Medium Range  
201    Weather Forecasts researchers and in the private sector. The accuracy of the WAM model's  
202    results is dictated by the accuracy in the bathymetric grid and wind forcing data used in the  
203    simulations.

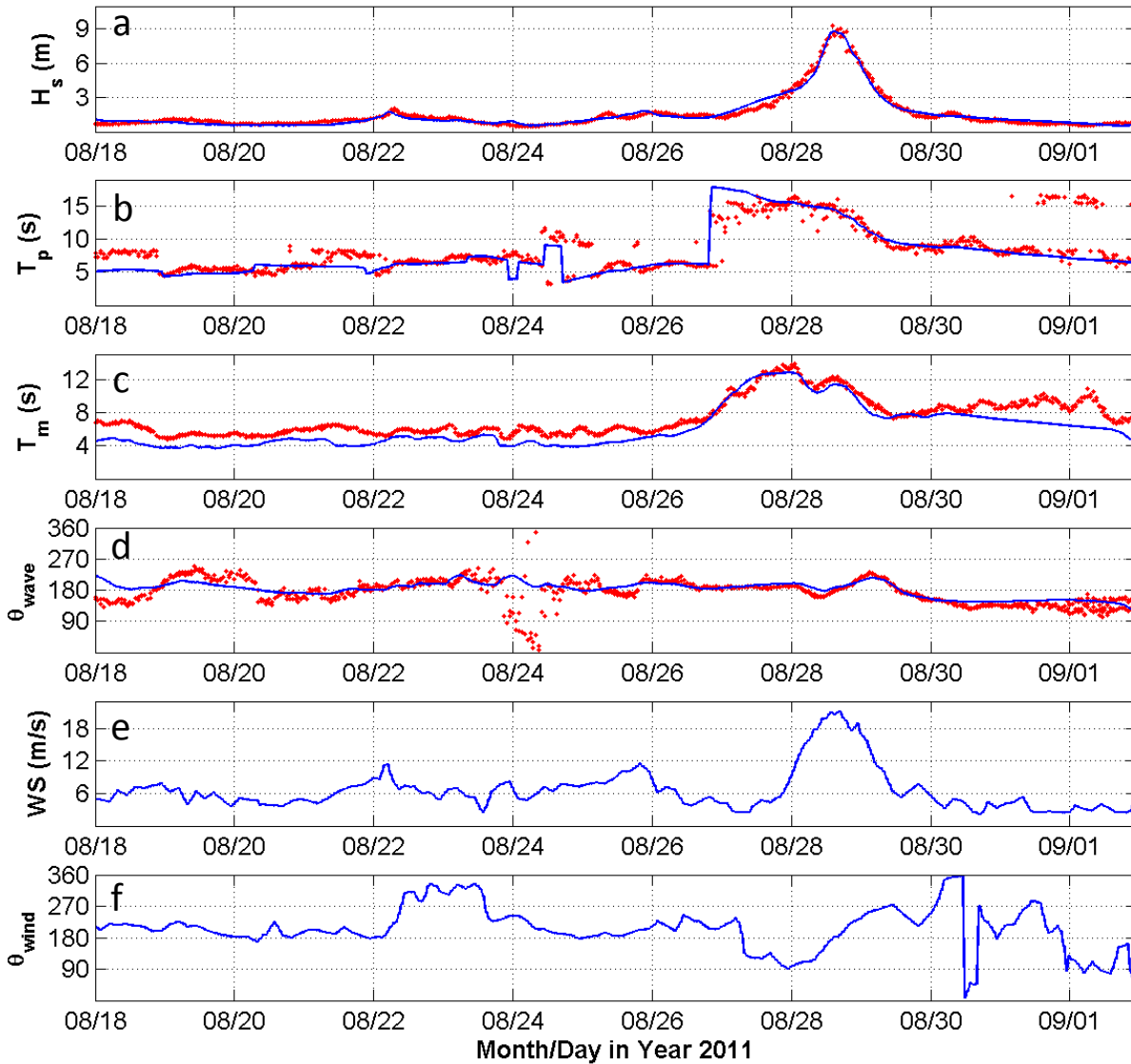
204  
205    The WAM results are used to provide spectral energy boundary conditions to the nearshore  
206    STWAVE model. This splitting up of waves between deep water and nearshore, allows for a  
207    more computationally efficient workflow for CSTORM and the use of wave models specifically  
208    designed for deep water and shallow water respectively. Since the WAM model uses a coarser  
209    spatial resolution than STWAVE and uses integer values for water depths, the WAM model is  
210    insensitive to changes in the geometry of the nearshore areas or water depth changes on the order  
211    of a meter or two. The STWAVE model, as most other nearshore wave models, is comparatively  
212    more computationally expensive than a 2D circulation model such as ADCIRC, and in general  
213    requires between 4 and 18 times the computational effort. As such, reducing the simulation  
214    region of the nearshore wave models, without significantly compromising nearshore results for  
215    waves and water levels, is desirable. Using the WAM model results to force the boundary of the  
216    STWAVE model allows swell propagating from far offshore to be included in the simulations,  
217    while reducing the computational time required by STWAVE. The WAM model setup used in  
218    this study is exactly the same as that used in the NACCS (Cialone et al., 2015, Jensen et al.,  
219    2016). Those reports provide significant details of the WAM model setup and validation results  
220    applied to several historical tropical and extra-tropical events, including Hurricane Irene. A  
221    sample of the WAM model result for Hurricane Irene are compared with measurement data at  
222    two NDBC buoys located near the study area, Station 44020 (Figure 5) and Station 44097  
223    (Figure 6). In the more open water areas around buoy 44097, the WAM results represent the

224 significant wave heights, peak and mean periods very well. However, buoy 44020 is located  
 225 near Nantucket and Martha’s Vineyard islands, including the Katama Bay system, and the WAM  
 226 model resolution is not designed specifically to capture them. This can be seen in the time series  
 227 (Figure 5), where the periods from the model indicate swells and the measurements indicate  
 228 wind-seas. Nevertheless, the model does well at reproducing the significant wave heights.  
 229



230  
 231 **Figure 5:** WAM model (blue curves) and NDBC buoy 44020 (red dots, “B” in Figure 3b) versus  
 232 time. a) significant wave height, b) peak period, c) mean period, d) wave direction, e) wind  
 233 speed, and f) wind direction.

234



235  
 236 **Figure 6:** WAM model (blue curves) and NDBC buoy 44097 (red dots, “A” in Figure 3b) versus  
 237 time. From top to bottom: significant wave height, peak period, mean period, wave direction, and  
 238 model only wind speed, and wind direction.

239

## 240 2.3 STEADY-STATE SPECTRAL WAVE MODEL

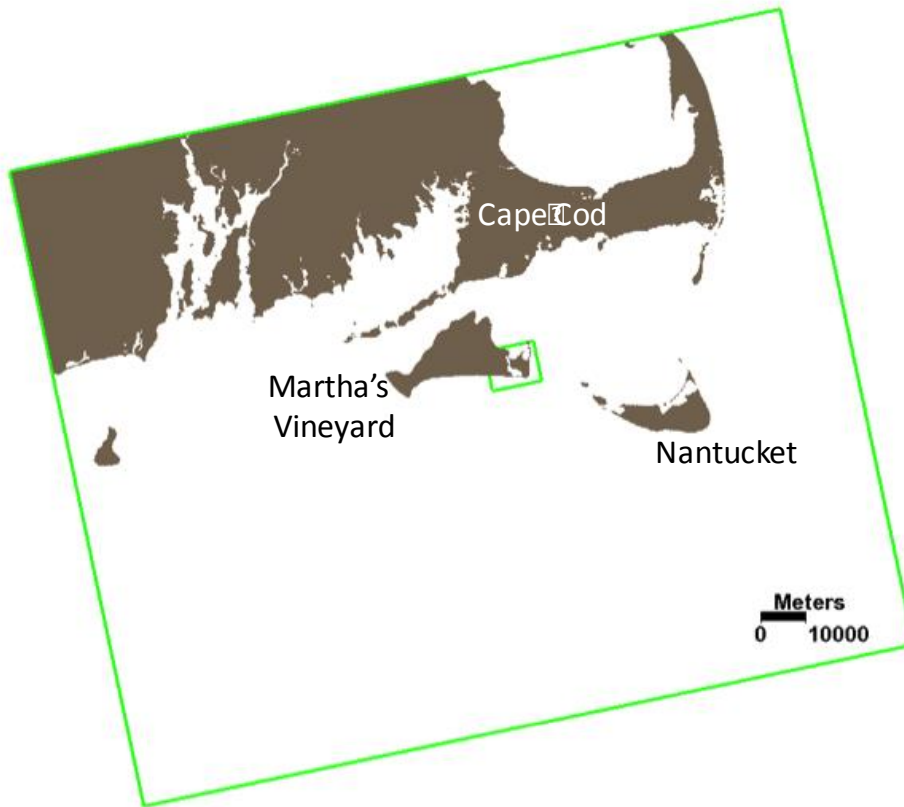
### 241 2.3.1 Model Description

242 STWAVE is a model developed by the United States Army Corps of Engineers to  
 243 estimate wind-wave growth and nearshore wave transformation, including shoaling, breaking,  
 244 diffraction, and refraction. STWAVE is a finite-difference, phase-averaged spectral model that  
 245 solves the wave action balance equation on a Cartesian, rectangular grid (Massey et al. 2011).

246 STWAVE is run in full-plane mode, which allows wave generation from all 360 degrees, and  
247 thus is better suited than half-plane mode for modeling waves during a hurricane. The steady-  
248 state STWAVE model operates under the assumption that the duration of meteorological forcing  
249 is not a limiting factor in the generation of wind waves over the domain.

### 250 **2.3.2 Model Setup and Domain**

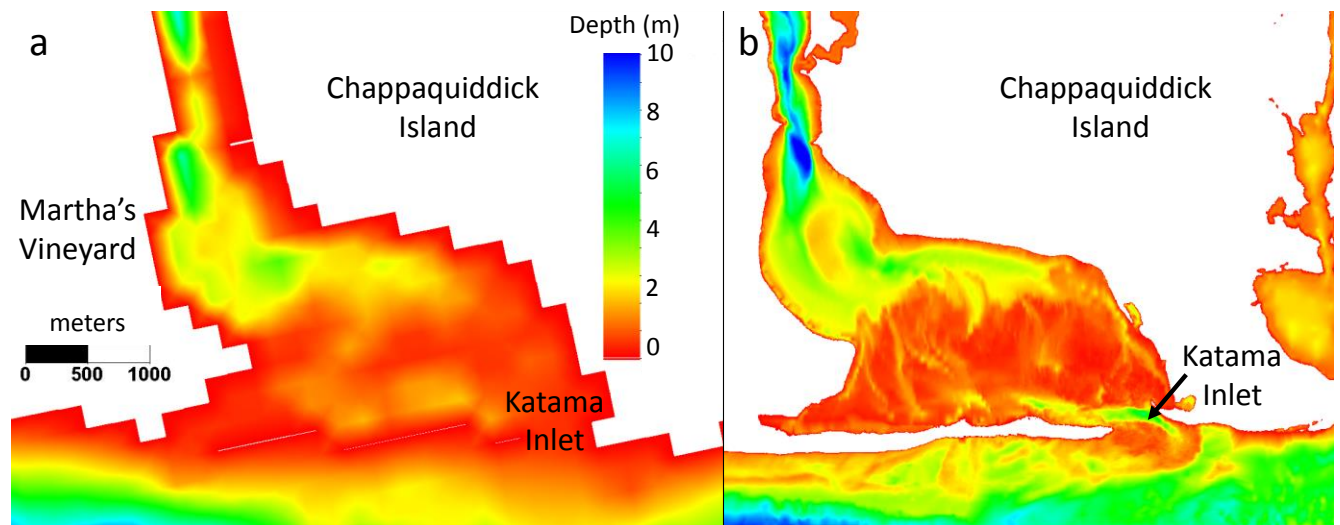
251 Two STWAVE grids are used here (Figure 7). A larger grid covering the southern  
252 Massachusetts (SMA) area developed for the North Atlantic Coast Comprehensive Study  
253 (NACCS) (Bryant and Jensen 2017) with a resolution of 200 by 200 m was used to generate  
254 wave spectra for boundary conditions for the smaller 10 by 10 m grid covering Katama Bay.  
255 Both grids were oriented at 101.5 degrees (Figure 7). Both models used 72 angle bands separated  
256 by 5 degrees and 30 frequency bands ranging from 0.04 to 0.33 Hz in increments of 0.01 Hz.  
257 The SMA grid has an origin  $(x_0, y_0)$  located at (465575.3, 4518084.4) in the UTM zone 19  
258 coordinate system measured in meters and is made up of 733 cells in the I-direction and 887 cells  
259 in the J-direction. The Katama Bay grid has an origin  $(x_0, y_0)$  located at (381625.68, 4577634.03)  
260 in the UTM zone 19 coordinate system measured in meters and is made up of 916 cells in the I-  
261 direction and 1134 cells in the J-direction. Waves on the NACCS SMA grid were forced with  
262 output from WAM and the (described above) Hurricane Irene wind fields. Morphic interpolation  
263 (Smith and Smith, 2002) of the directional spectra was used along the boundary of both  
264 STWAVE grids to supply spectral energy inputs to the models, and both models used wave  
265 breaking. Independent STWAVE simulations with a static water elevation were run from August  
266 27 to August 30, 2011 to include the effects of Hurricane Irene, which produced a peak surge in  
267 the research area on the afternoon of August 28, 2011. Model time steps, or snaps, were set at  
268 every 30 minutes. Bathymetry values for the SMA grid were interpolated from the NACCS  
269 ADCIRC mesh, which combined numerous sources to obtain the most accurate bathymetry  
270 possible (see Cialone et al. 2015, 2017 for model development discussion and details).



271

272 **Figure 7:** The Southern Massachusetts grid (SMA) (outer green box) and the higher-spatial  
 273 resolution Katama Bay grid (KB) (inner green box) used for STWAVE.

274 Bathymetry for the high-resolution Katama Bay (KB) grid was obtained from surveys conducted  
 275 with GPS- and sonar-equipped small boats combined with a 10-m resolution digital elevation  
 276 model produced by NOAA in 2008 (Orescanin et al. 2016). The Katama Bay grid resolves the  
 277 smaller-scale bathymetric contours of the bay and offshore region, particularly in the vicinity of  
 278 the inlet and ebb shoal, in contrast to the lower-resolution SMA grid (Figure 8). Prior to  
 279 coupling, both nested (Smith and Smith 2002) and un-nested STWAVE model runs conducted  
 280 for the Hurricane Irene time period using the high-resolution grid were stable. For the large-  
 281 scale, un-nested-grid case, there were no waves specified on the southern boundary, with waves  
 282 generated within the grid using the OWI Hurricane Irene wind field. When using the nested  
 283 grids, waves on the boundaries of the inner, high-resolution grid were provided by the spectral  
 284 output from the SMA grid.



285

286 **Figure 8:** Contours of bathymetry (color and scale bars are in (a)) for a) the 200 by 200 m  
 287 coarse SMA STWAVE grid and b) the 10 by 10 m fine Katama Bay (KB) STWAVE grid.

## 288 2.4 CIRCULATION MODEL

### 289 2.4.1 Model Description

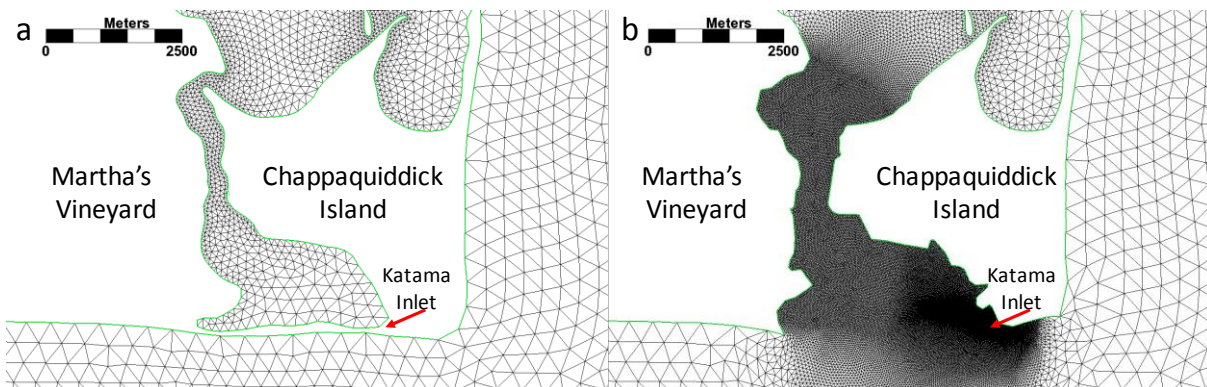
290 The two-dimensional variant of the Advanced Circulation model (ADCIRC) is a depth-  
 291 averaged model for ocean circulation based on the shallow water equations for conservation of  
 292 mass and momentum, and applies Boussinesq and hydrostatic pressure approximations (Luettich  
 293 et al. 1992; Westerink et al. 1992). ADCIRC is an unstructured finite-element model, and thus  
 294 the resolution can be varied across the domain to resolve complex bathymetry and associated  
 295 processes in areas of interest, while minimizing computational cost by relaxing the resolution in  
 296 areas where the bathymetry varies more slowly.

### 297 2.4.2 Model Setup and Domain

298 Two ADCIRC meshes of differing resolution were used (Figure 9). The coarser mesh  
 299 was taken from the NACCS (Cialone et al., 2015; 2017). The finer mesh was developed by  
 300 merging the Katama Bay mesh (Orescanin et al. 2016) with the NACCS mesh to achieve the  
 301 resolution required near the coast and within the bay, while simultaneously including the large,  
 302 basin-scale effects crucial to model storm surge accurately (Blain et al. 1994), here called the  
 303 KB-ADCIRC mesh. The NACCS mesh treats the southern shoreline of Martha's Vineyard  
 304 (Figures 1, 3) as a hard, no normal-flow boundary (Figure 9a), whereas the high-resolution KB-

305 ADCIRC mesh allows water to overtop the low-elevation Norton Point (Figure 1, 3b) and to  
306 enter Katama Bay through Katama Inlet (Figure 9b). Tidal forcing was applied to both meshes at  
307 the open ocean boundaries near 60 degrees west longitude. Consistent with the STWAVE grids,  
308 meteorological forcing was applied from Oceanweather Hurricane Irene wind and pressure  
309 fields. The ADCIRC simulations were run for a period of 24 days consisting of a 14-day tidal  
310 spin-up before winds were applied to the domain from August 20 to August 30, 2011. The  
311 Courant-limited time step for ADCIRC model runs was 0.5 seconds. A constant water level  
312 adjustment (the “sea surface height above geoid” parameter in ADCIRC) was set to the NACCS  
313 value of 0.111 meters to represent baroclinic and steric effects not accounted for in the ADCIRC  
314 model (Cialone et al. 2015). Values for spatially varying bottom friction, horizontal eddy  
315 viscosity, and primitive equation weighting of the continuity equation were the same as those in  
316 the NACCS study (Cialone et al. 2015). Manning’s n was set to the NACCS values, except for  
317 the areas in the higher-resolution area of the ADCIRC mesh, where the Manning’s n values were  
318 reset to those used in a previous study (Orescanin et al. 2016). Additional ADCIRC model input  
319 parameters include a nonlinear bottom friction with finite amplitude terms and a lower limit of  
320 bottom friction (FFACTOR) of 0.003, nonlinear advection terms in space and time, a 2.0-day  
321 ramp period using the hyperbolic tangent ramping function, a wetting and drying threshold depth  
322 of 0.10 meters, and a minimum wetting velocity of 0.10 m/s.

323



324

325 **Figure 9:** a) The NACCS mesh and b) the NACCS and Katama merged ADCIRC mesh.



## 326 **2.5 MODEL COUPLING**

327 To simulate surge levels, wind waves, currents, and the interactions among them,  
328 ADCIRC and STWAVE were two-way coupled in water level and wave-radiation stresses using  
329 the Coastal Storm Modeling System (CSTORM-MS) coupler (Massey et al. 2011). This coupling  
330 enables ADCIRC to pass water levels and current velocities to STWAVE and to receive wave  
331 radiation-stress gradients during run time at every STWAVE snap (every 30 minutes). With this  
332 coupling, wind blowing over inundated regions during high surge events will generate waves.  
333 Both ADCIRC and STWAVE were run in their parallel computing modes by partitioning the  
334 domain to utilize high-performance computing resources at the Hamming cluster at the Naval  
335 Postgraduate School and the Topaz SGI system at the United States Army Corps of Engineers  
336 High Performance Computing Center. The three models compared here are the (1) NACCS  
337 coarse resolution coupled model (NACCS), (2) the high resolution ADCIRC-only model (KB-  
338 ADCIRC), and (3) the high resolution coupled model (KB-CSTORM).

339

## 340 **3 RESULTS AND DISCUSSION**

### 341 **3.1 OBSERVATIONAL DATA**

342 To assess the accuracy of the models, comparisons were made with observations during  
343 Hurricane Irene in Katama Bay. Water elevation was estimated with bottom-mounted pressure  
344 sensors (sampled at 2 Hz) along the north-south axis of the bay (yellow circles, Stations 01-03,  
345 Figure 1). Station 01, the northern most station is near the transition from the bay to Vineyard  
346 Sound through Edgartown Channel. Station 02 is the farthest from any land boundary  
347 interaction and characterizes Katama Bay. Station 03 is close to Katama Inlet, near the transition  
348 from the Atlantic Ocean to Katama Bay. More details of the observations can be found in  
349 Orescanin et al. 2014. Model results also were output at 10 additional locations within the bay, as  
350 well as on the ebb shoal (Station 04) to simulate conditions outside of the bay.

351 **3.2 MODEL EVALUATION**

352 **3.2.1 Error Statistics**

353 As is seen in many storm surge modeling efforts (Orton et al. 2012; Sun et al. 2013),  
 354 modeled water-elevation levels were less than observed, with the maximum under prediction  
 355 during peak surge (Figure 2c and d). Water level is predicted more accurately by the models that  
 356 use high spatial-resolution meshes (KB-ADCIRC and KB-CSTORM) than by the lower  
 357 resolution NACCS model (Figure 2 and Table 1). The high-resolution model (KB-ADCIRC and  
 358 KB-CSTORM) predictions of the timing of the peak storm surge are more accurate than the  
 359 NACCS predictions, which tend to lag the observed peak surge (Figure 2). The coupled KB-  
 360 CSTORM has somewhat lower errors than KB-ADCIRC at the center (Figure 2d, Station 02)  
 361 and southern side (Figure 2e, Station 03) of the bay, particularly during the 12-hour period of  
 362 peak storm surge (Figure 2 and Table 1 column 4). The 12-hour period was selected to represent  
 363 the shortest duration of peak storm and provides an end-member estimate of reduction of error  
 364 (the RMSE will be bounded by the typical conditions and peak storm duration). The reduction in  
 365 error percentage by coupling with the wave model is small during calm conditions, but increases  
 366 during the peak surge period, suggesting that both bottom topography and waves are important to  
 367 modeling hydrodynamics near inlets.

368 Table 1. Root mean square error between modeled and observed water levels for the total  
 369 duration time series (column 3) and for the 12-hour window centered on the time of the  
 370 peak surge (Storm Duration, column 4).

Station	Model	Total Timeseries RMSE (m)	Storm Duration RMSE (m)
01	NACCS	0.18	0.27
	KB-ADCIRC	0.18	0.30
	KB-CSTORM	0.17	0.24
02	NACCS	0.16	0.31
	KB-ADCIRC	0.15	0.28
	KB-CSTORM	0.13	0.19
03	NACCS	0.22	0.33
	KB-ADCIRC	0.08	0.16
	KB-CSTORM	0.10	0.19
Average	NACCS	0.19	0.30
	KB-ADCIRC	0.14	0.25
	KB-CSTORM	0.13	0.21

371

372 Table 2. Error reduction relative to the low-spatial resolution NACCS results. Reduction  
373 is defined as  $(RMSE\_NACCS - RMSE\_KBXX) / RMSE\_NACCS * 100\%$  from the  
374 Average values (bottom rows in Table 1).

<b>Model</b>	<b>Total Timeseries Error Reduction (%)</b>	<b>Storm Duration Error Reduction (%)</b>
<b>KB-ADCIRC</b>	26.3	16.7
<b>KB-CSTORM</b>	31.6	30.0

375

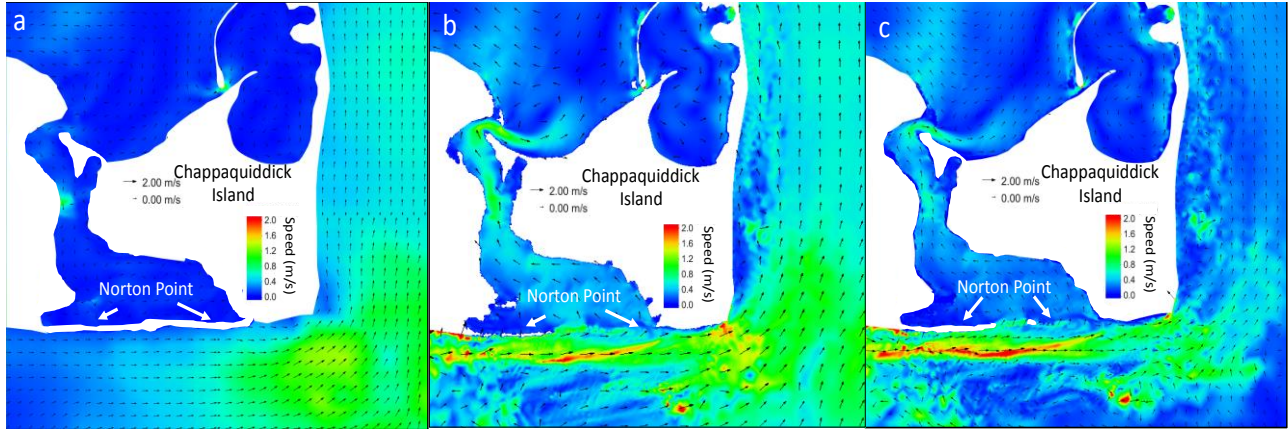
## 376 **3.2.2 Spatial Comparisons**

### 377 *3.2.2.1 Resolution Effects*

378 Increasing spatial resolution leads to more accurate modeled values. However, another  
379 explanation for the difference in accuracy between the NACCS and the high-resolution runs is  
380 that during NACCS mesh development, the southern shoreline (Norton Point, Figures 1, 3a) is  
381 made into a hard no-normal-flow boundary. The result is that NACCS does not allow flow  
382 through Katama Inlet nor the overtopping of the beach that occurred during Hurricane Irene. The  
383 lack of inlet currents and of overtopping can explain many of the flow-pattern differences  
384 between the high-resolution models and the NACCS. The NACCS does not allow Atlantic water  
385 to enter Katama Bay from the south, and thus the simulated circulation (Figure 10a, NACCS)  
386 and water levels (Figure 2, NACCS) in the bay are owing to wind stress and to water entering or  
387 exiting through Edgartown Channel to the north, in contrast with the high-resolution models  
388 (Figures 5, 6b, KB-CSTORM) and with the observations during peak surge conditions. In  
389 addition, the high-resolution models indicate a narrow coastal jet with magnitudes over 2.0 m/s  
390 along the southern coast that is not apparent in the lower-resolution simulations. Currents also  
391 are amplified within the Bay and Edgartown Channel relative to those simulated with NACCS  
392 (compare Figures 10b and c with Figure 10a), indicating a net northward circulation, consistent  
393 with previous results (Orescanin et al., 2014). Comparing the effects of resolution and waves on  
394 velocity during peak surge suggests not only increased northward flow through Katama Bay for

395 KB-ADCIRC (Figure 10b) and KB-CSTORM (Figure 10c), but also an enhanced coastal current  
396 during KB-CSTORM compared with KB-ADCIRC, suggesting the influence of waves is to  
397 concentrate flows along the coast.

398



399

400 **Figure 10:** Contours of current speed (color bars are inset) and vectors (point in direction  
401 of the current with length proportional to speed, scale left of and above the color bars) for  
402 a) NACCS b) KB-ADCIRC and c) KB-CSTORM during peak surge. Norton Point is  
403 indicated by arrows.

404

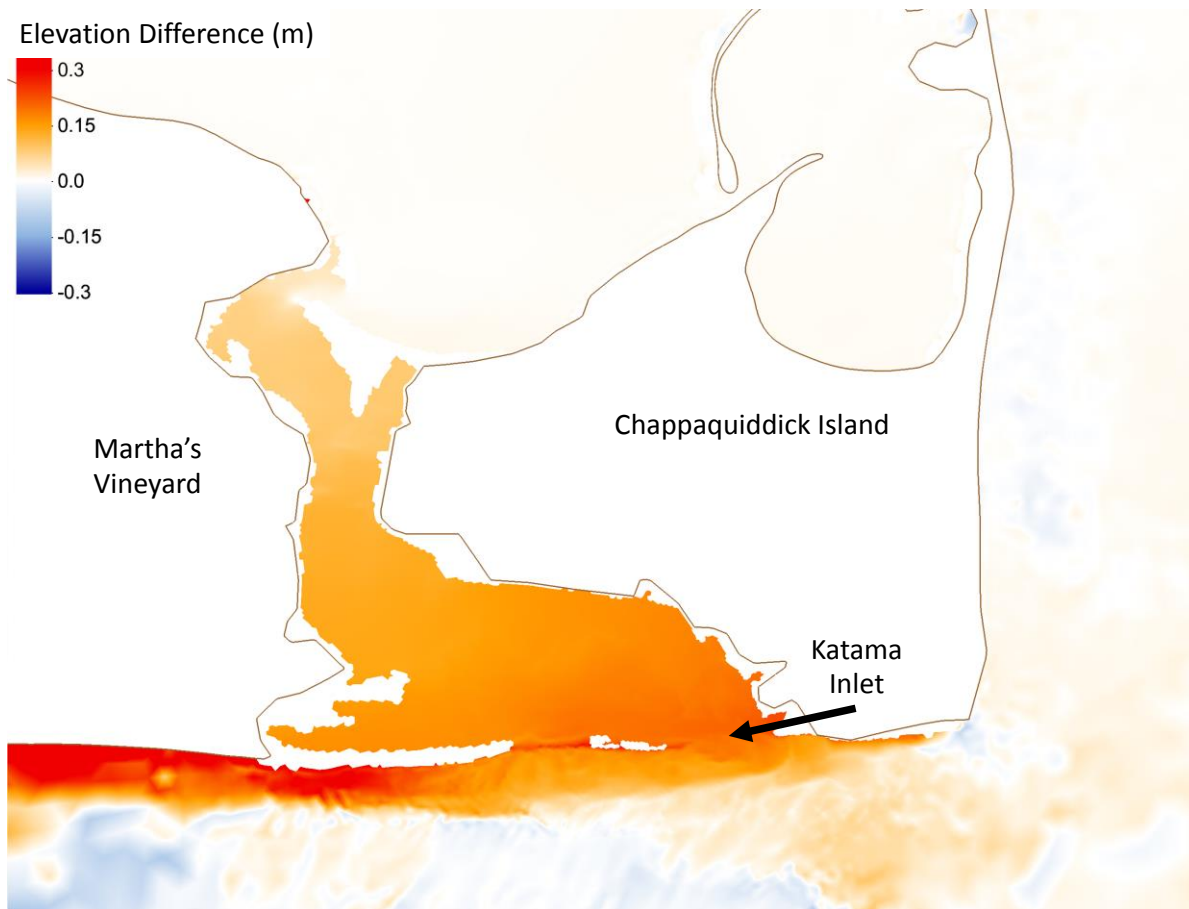
405 During the peak surge the NACCS model tends to have higher water levels on the  
406 southern shoreline than either of the high-resolution models (Figure 2f). The ~0.3 m increase in  
407 NACCS modeled water level suggests that the high-resolution bathymetry that includes the  
408 relatively small Katama Inlet may have a relatively large effect on shoreline water levels. In  
409 addition, the predicted increase in surge on the southern shore simulated by the low-resolution  
410 model with no inlet suggests a possibility of enhanced overtopping along Norton Point when the  
411 inlet is closed, consistent with the observation that Katama Inlet opens during extreme surge  
412 events.

### 413 **3.2.2.2 Coupling Effects**

414 Error statistics show that the coupling of STWAVE and ADCIRC in KB-CSTORM  
415 improves prediction performance compared with using ADCIRC alone (KB-ADCIRC),  
416 especially on the southern shore and within Katama Bay. For example, during the peak storm  
417 surge, KB-CSTORM includes wave-driven setup, and predicts significantly (up to 0.3 m) higher

418 water elevations in the southern part of Katama Bay and in the surf zone directly to the south  
419 than are predicted by KB-ADCIRC (Figure 11). In addition, the overall higher water levels  
420 within Katama Bay predicted by KB-CSTORM during peak surge indicates waves are  
421 contributing to an overall elevation change within the bay, consistent with previous results for  
422 single-inlet systems (Malhadas et al., 2009; Olabarrietta et al., 2011). Although the more  
423 common moderate wave forcing may not increase the bay water levels (Orescanin et al., 2014),  
424 during surge events not all wave-driven momentum flux entering the bay through Katama Inlet  
425 can be radiated out of the bay through Edgartown Channel, resulting in an overall bay setup that  
426 is common in single-inlet systems.

427           Currents simulated by the higher-resolution KB-ADCIRC and KB-CSTORM models  
428 have tidal fluctuations throughout the Bay in contrast to the weaker (and non-tidal) velocities  
429 predicted by the coarser NACCS model (not shown). KB-ADCIRC and KB-CSTORM  
430 velocities are nearly identical during calm wave conditions, but deviate during Irene, with KB-  
431 CSTORM predicting a reduced ebb current (to zero flow) during the peak of the storm,  
432 consistent with the breaking-wave-driven currents observed at Katama Inlet (Orescanin, et al,  
433 2014).

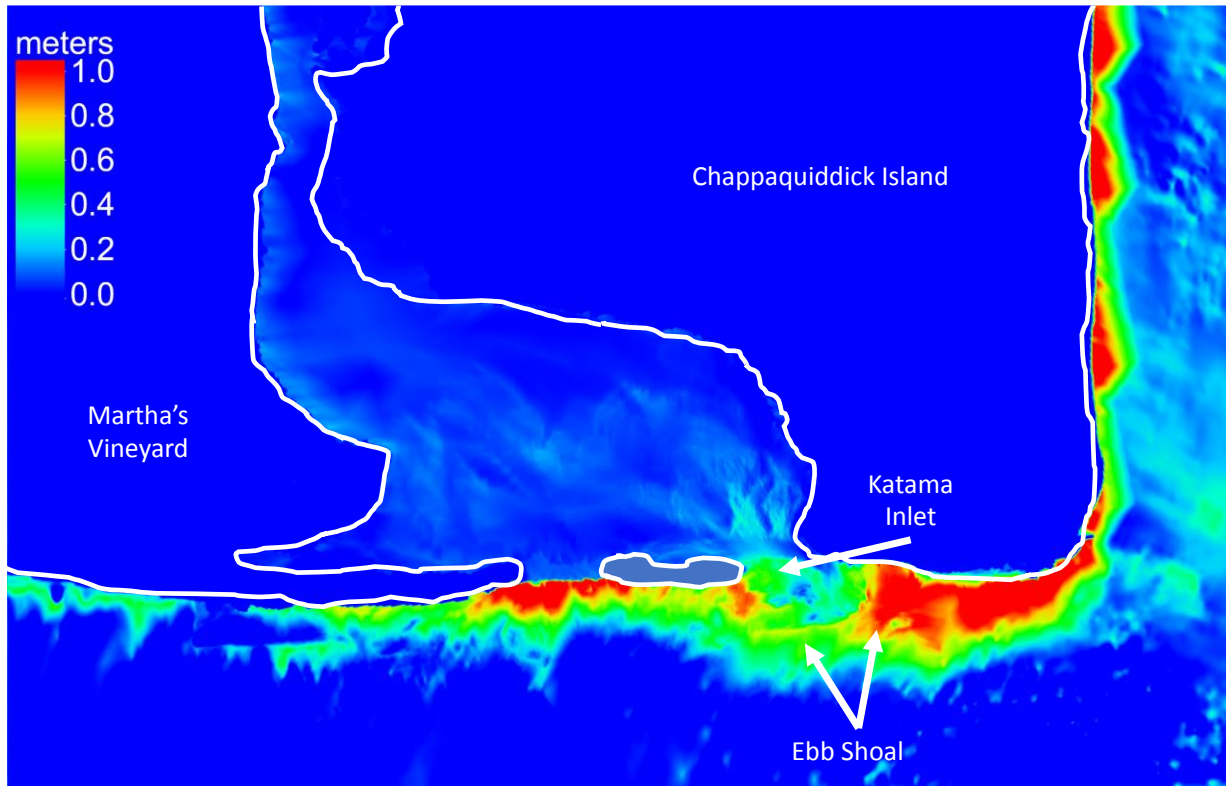


434

435 **Figure 11:** Contours (color bar in the upper left) of water elevation difference between  
 436 KB-CSTORM and KB-ADCIRC model runs during peak storm surge.

437         At some locations, KB-CSTORM predicts much larger ( $> 1$  m) significant wave heights  
 438 than NACCS predicts, especially near the shore (Figure 12). Both models predicted  $\sim 0.5$  m wave  
 439 height in the center of the bay (Figure 1, Station 02) during the peak of the storm, in contrast to  
 440 the observed  $\sim 0.2$  m wave height (not shown). On the ebb shoal (Figure 1, Station 04, just  
 441 offshore off the mouth of Katama Inlet) NACCS predicts much smaller wave heights than KB-  
 442 CSTORM predicts (Figure 12). There were no observations on the ebb shoal, but comparisons of  
 443 model predictions with observations of waves in 12 m depth, a few km south of the ebb shoal  
 444 (Martha's Vineyard Coastal Observatory, <https://www.whoi.edu/mvco>, not shown) suggest the  
 445 modeled wave heights are similar to those observed (up to 5 m significant wave height) before  
 446 and after the peak of the storm (the MVCO sensor did not operate for a few hours during the  
 447 peak of the storm). The KB-CSTORM model predicts  $\sim 3$  m wave heights on the ebb shoal  
 448 during the peak of the storm, whereas the NACCS model predicts 1.5 m wave heights The

449 underprediction of wave heights by NACCS (red colors near the ebb shoal, Figure 12) may be  
450 related to the low-resolution bathymetry or to the lack of two-way coupling with the wave  
451 model.



452  
453 **Figure 12:** Contours (color bar in upper left) of wave height difference between KB-  
454 CSTORM and NACCS model runs during peak storm surge.

## 455 4 CONCLUSIONS

456 Comparisons of simulations with observations in the Katama Bay system prior to and  
457 during Hurricane Irene indicate that the coupling of wave (STWAVE) with circulation  
458 (ADCIRC) models in addition to using high resolution bathymetry (KB-CSTORM) results in  
459 better predictions of wave heights and water levels during Hurricane Irene than predicted with  
460 the lower resolution (KB-NACCS) or with the high resolution, no wave (KB-ADCIRC) models.  
461 These results suggest that both high spatial resolution of small (< 400 m) tidal inlets and wave  
462 coupling are required for accurate surge prediction. During the peak surge of Hurricane Irene,  
463 errors in water level elevations were 30% lower using KB-CSTORM than using NACCS. The  
464 improved model predictions primarily are owing to resolving the inlet and nearby shorelines in  
465 the KB-CSTORM model, whereas the low-spatial resolution NACCS does not include the inlet  
466 nor does it allow overwash of the sand barrier separating Katama Bay from the ocean. An artifact  
467 of the low-resolution bathymetry is higher water levels and smaller currents along the shoreline  
468 than predicted by KB-CSTORM, which could lead to inaccurate predictions of sediment  
469 transport and morphological change.

470 Prior studies during moderate wave conditions show that water driven into Katama Bay  
471 by breaking-wave-induced momentum flux leaves the bay through Edgartown Channel, and thus  
472 bay water levels do not increase. In contrast, during extreme events (e.g., Hurricane Irene),  
473 model simulations suggest the flux through Edgartown Channel is insufficient to balance the  
474 breaking-wave-induced increased flows into Katama Bay through Katama Inlet, resulting in an  
475 increased water elevation in the bay. The increased water levels within the bay during storms can  
476 result in relatively large waves that could erode the banks and flood surrounding marshes.

### 477 **Acknowledgements:**

479  
480 We thank Levi Gorrell and the PVLAB field crew for deploying, maintaining, and recovering  
481 sensors in sometimes less-than-ideal conditions. Thanks to MVCO for wave height and wind  
482 velocity time series. Funding was provided by a Vannevar Bush Faculty Fellowship  
483 (OUSD(R&E)), Sea Grant, NSF, and ONR.



## LIST OF REFERENCES

- 485 Baugh, J., Altuntas, A., Dyer, T., Simon, J., 2015. An exact reanalysis technique for storm surge  
486 and tides in a geographic region of interest. *Coast. Eng.*, 97, 60-77,  
487 doi:10.1016/j.coastaleng.2014.12.003.
- 488 Bennett, V.C., Mulligan, R.P. and Hapke, C.J., 2018. A numerical model investigation of the  
489 impacts of Hurricane Sandy on water level variability in Great South Bay, New York.  
490 *Continental Shelf Research*, 161, pp.1-11.
- 491 Bertin, X., Fortunato, A.B. and Oliveira, A., 2009. A modeling-based analysis of processes  
492 driving wave-dominated inlets. *Continental Shelf Research*, 29(5-6), pp.819-834.
- 493 Blain, C.A., Westerink, J. J., Luettich Jr, R.A., 1994. The influence of domain size on the  
494 response characteristics of a hurricane storm surge model. *J. of Geophys. Res., Oceans*  
495 99, 18467, doi:10.1029/94JC01348.
- 496 Blake, E.S., Rappaport, E.N., Jarrell, J.D., Landsea, C.W., 2007. The deadliest, costliest and  
497 most intense United States hurricanes from 1851 to 2004 (and other frequently requested  
498 hurricane facts). NOAA, Technical Memorandum NWS-TPC-5, 48 pp.
- 499 Bryant, M. A., Jensen, R. E., 2017. Application of the nearshore wave model STWAVE to the  
500 North Atlantic coast comprehensive study. *J. of Waterway, Port, Coast. and Ocean*
- 501 Chen, C., Beardsley, R.C., Cowles, G., Qi, J., Lai, Z., Gao, G., Stuebe, D., Liu, H., Xu, Q., Xue,  
502 P., Ge, J., Ji, R., Hu, S., Tian, R., Huang, H., Wu, L., Lin, H., Sun, Y., Zhao, L., 2013. An  
503 Unstructured-Grid, Finite-Volume Community Ocean Model FVCOM User Manual,  
504 third ed., SMAST/UMASSD Tech. Rep.-13-0701. Univ. of Mass.-Dartmouth, New  
505 Bedford, Massachusetts, pp. 404. *Eng.*, 143, 4017026, doi:10.1061/(ASCE)WW.1943-  
506 5460.0000412.
- 507 Cialone, M. A., Massey, T. C., Anderson, M. E., Grzegorzewski, A. S., Jensen, R. E., Cialone,  
508 A., Mark, D. J., Pevey, K. C., Gunkel, B. L., McAlpin, T. O., 2015. North Atlantic Coast  
509 Comprehensive Study (NACCS) Coastal Storm Model Simulations: Waves and Water  
510 Levels. ERDC/CHL TR-15-14. Vicksburg, MS: U.S. Army Engineering Research and  
511 Development Center.
- 512 Cialone, M. A., Grzegorzewski, A. S., Mark, D. J., Bryant, M. A., Massey, T. C., 2017. Coastal-  
513 storm model development and water-level validation for the North Atlantic coast  
514 comprehensive study. *J. of Waterway, Port, Coast. and Ocean Eng.*, 143, 4017031,  
515 doi:10.1061/(ASCE)WW.1943-5460.0000408.
- 516 Dietrich, J., Tanaka, S., Westerink, J., Dawson, C., Luettich Jr, R., Zijlema, M., Holthuijsen, L.,  
517 Smith, J., Westerink, L., Westerink, H., 2012. Performance of the Unstructured-Mesh,  
518 SWAN+ADCIRC Model in Computing Hurricane Waves and Surge. *J. of Sci.*  
519 *Comp.*, 52, 468–497, doi:10.1007/s10915-011-9555-6.

- 520 Dodet, G., Bertin, X., Bruneau, N., Fortunato, A. B., Nahon, A., and Roland, A., 2013. Wave-  
521 current interactions in a wave- dominated tidal inlet, *J. Geophys. Res. Oceans*, 118,  
522 1587– 1605, doi: 10.1002/jgrc.20146.
- 523 Gonçalves, M., Rusu, E., Guedes Soares, C., 2015. Evaluation of two spectral wave models in  
524 coastal areas. *J. of Coast. Res.*, 31, 326–339, doi:10.2112/JCOASTRES-D-12-00226.1.
- 525 Hopkins, J., Elgar, S., Raubenheimer, B., 2017. Flow separation effects on shoreline sediment  
526 transport. *Coast. Eng.*, 125, 23–27, doi:10.1016/j.coastaleng.2017.04.007.
- 527 Hopkins, J., Elgar, S., Raubenheimer, B., 2016. Observations and model simulations of wave-  
528 current interaction on the inner shelf. *J. of Geophys. Res.: Oceans*, 121, 198–208,  
529 doi:10.1002/2015JC010788.
- 530 Jensen, R. & Cialone, A. & Smith, Jane & Bryant, M. & Hesser, Tyler. (2016). Regional Wave  
531 Modeling and Evaluation for the North Atlantic Coast Comprehensive Study. *Journal of*  
532 *Waterway, Port, Coastal, and Ocean Engineering*. 143. B4016001.  
533 10.1061/(ASCE)WW.1943-5460.0000342.
- 534 Kang, X. and Xia, M., 2020. The Study of the Hurricane-Induced Storm Surge and Bay-Ocean  
535 Exchange Using a Nesting Model. *Estuaries and Coasts*, pp.1-15.
- 536 Kerr, P. C., Martyr, R. C., Donahue, A. S., Hope, M. E., Westerink, J. J., Luettich, R. A.,  
537 Kennedy, A. B., Dietrich, J. C., Dawson, C., Westerink, H. J., 2013: U.S. IOOS coastal  
538 and ocean modeling testbed: Evaluation of tide, wave, and hurricane surge response  
539 sensitivities to mesh resolution and friction in the Gulf of Mexico. *J. of Geophys. Res.:*  
540 *Oceans*, 118, 4633–4661, doi:10.1002/jgrc.20305.
- 541 Komen, G.J. L. Cavaleri, M. Donelan, K. Hasselmann, S. Hasselmann, and P.A.E.M. Janssen,  
542 (1994). *Dynamics and modeling of ocean waves*. Cambridge University Press, United  
543 Kingdom. 532 pp.
- 544 Kumar, N., Voulgaris, G., Warner, J.C., 2011. Implementation and modification of a three-  
545 dimensional radiation stress formulation for surf zone and rip-current applications. *Coast.*  
546 *Eng.* 58, 12, 1097-1117, <https://doi.org/10.1016/j.coastaleng.2011.06.009>.
- 547 Lawler, S., Haddad, J. and Ferreira, C.M., 2016. Sensitivity considerations and the impact of  
548 spatial scaling for storm surge modeling in wetlands of the Mid-Atlantic region. *Ocean &*  
549 *Coastal Management*, 134, pp.226-238.
- 550 Luettich, R. A., Jr., Westerink, J.J., Scheffner, N.W., 1992. ADCIRC: An advanced three-  
551 dimensional circulation model for shelves, coasts, and estuaries. Tech. Rep. DRP-92-6,  
552 U.S. Army Engineer Research and Development Center, Vicksburg, MS.
- 553 Malhadas, M., Leitao, P., Silva, A., Neves, R., 2009. Effect of coastal waves on sea level in  
554 Obidos Lagoon, Portugal. *Cont. Shelf Res.*, 29, 1240–1250.

555 Mao, M. and Xia, M., 2018. Wave–current dynamics and interactions near the two inlets of a  
556 shallow lagoon–inlet–coastal ocean system under hurricane conditions. *Ocean Modelling*,  
557 129, pp.124-144.

558 Massey, T. C., Anderson, M.E., Smith, J.M., Gomez, J., Jones, R., 2011. STWAVE: Steady-state  
559 spectral wave model user’s manual for STWAVE, Version 6.0. ERDC/CHL SR-11-  
560 1.U.S. Army Engineer Research and Development Center, Vicksburg, MS.

561 Massey, T.C., Wamsley, T.V., Cialone, M.A., 2011. Coastal Storm Modeling – System  
562 Integration. Proceedings of the 2011 Solutions to Coastal Disasters Conference,  
563 Anchorage, Alaska, 99-108.

564 Neumann, J., Emanuel, K., Ravela, S., Ludwig, L., Kirshen, P., Bosma, K., Martinich, J., 2015.  
565 Joint effects of storm surge and sea-level rise on U.S. Coasts: new economic estimates of  
566 impacts, adaptation, and benefits of mitigation policy. *Climatic Change*, 129, 337–349,  
567 doi:10.1007/s10584-014-1304-z.

568 Olabarrieta, M., Warner, J., Kumar, N., 2011. Wave–current interaction in Willipa Bay. *J. of*  
569 *Geophys. Res.: Oceans*, 116, C12014, doi:10.1029/2011JC007387.

570 Orescanin, M., Raubenheimer, B., Elgar, S., 2014. Observations of wave effects on inlet  
571 circulation. *Cont. Shelf Res.*, 82, 37–42, doi:10.1016/j.csr.2014.04.010.

572 Orescanin, M., Elgar, S., Raubenheimer, B., 2016. Changes in bay circulation in an evolving  
573 multiple inlet system. *Cont. Shelf Res.*, 124, 13–22, doi:10.1016/j.csr.2016.05.005.

574 Orton, P., Georgas, N., Blumberg, A., Pullen, J. 2012. Detailed modeling of recent severe storm  
575 tides in estuaries of the New York City region. *J. of Geophys. Res.: Oceans*, 117,  
576 doi:10.1029/2012JC008220.

577 OWI (Oceanweather, Inc.), 2015. Development of wind and pressure forcing for the North  
578 Atlantic Coast Comprehensive Study (NACCS). Contractor Rep. submitted to the U.S.  
579 Army Engineer, Engineer Research and Development Center, Stamford, CT.

580 Smith, J. M., Smith, S.J., 2002. Grid nesting with STWAVE, ERDC/CHL CHETN I-66, U.S.  
581 Army Engineer Research and Development Center, Vicksburg, MS.

582 Sun, Y., Chen, C., Beardsley, R. C., Xu, Q., Qi, J., Lin, H., 2013. Impact of current-wave  
583 interaction on storm surge simulation: A case study for Hurricane Bob. *J. of Geophys.*  
584 *Res.: Oceans*, 118, 2685–2701, doi:10.1002/jgrc.20207.

585 SWAN Team (2017). Scientific and Technical Documentation for SWAN Cycle III version  
586 41.20. Technical report from Delft University of Technology.  
587

588 Tolman, H.L. (2014). User manual and system documentation of WAVEWATCH III Version  
589 4.18. Technical Note. U.S. Department of Commerce., MMAB Contribution no 316.  
590

- 591 WAMDI Group, 1998. The WAM Model—A third generation ocean wave prediction model. *J.*  
592 *of Phys. Ocean.*, 18, 1775-1810.
- 593 Yin, J., Lin, N., Yu, D., 2016. Coupled modeling of storm surge and coastal inundation: A case  
594 study in New York City during Hurricane Sandy. *Water Resources Res.*, 52, 8685–8699,  
595 doi:10.1002/2016WR019102.

Figure 1



Figure 2

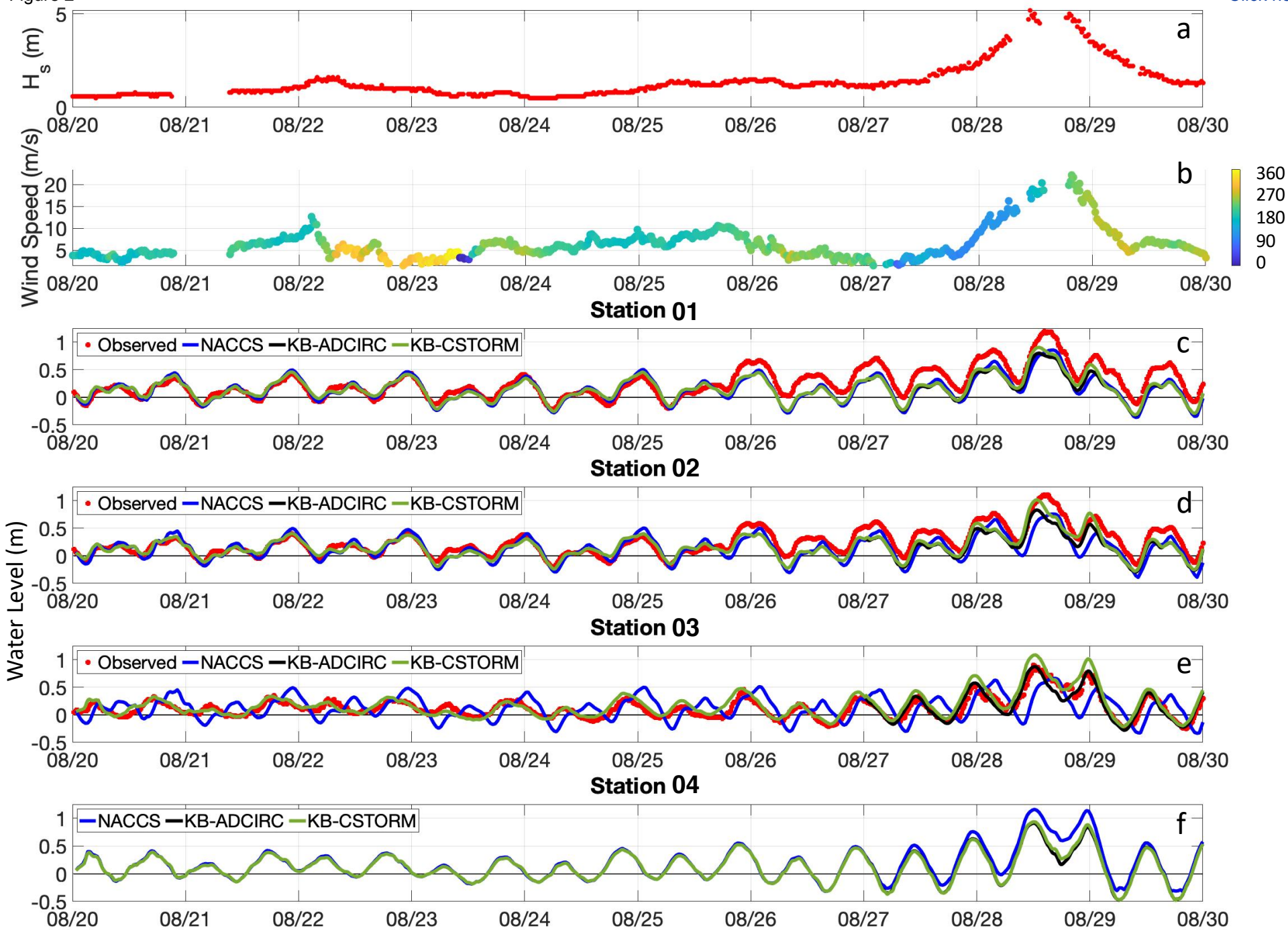
[Click here to access/download;Figure;Figure2\\_TS\\_V2.pdf](#)

Figure 3

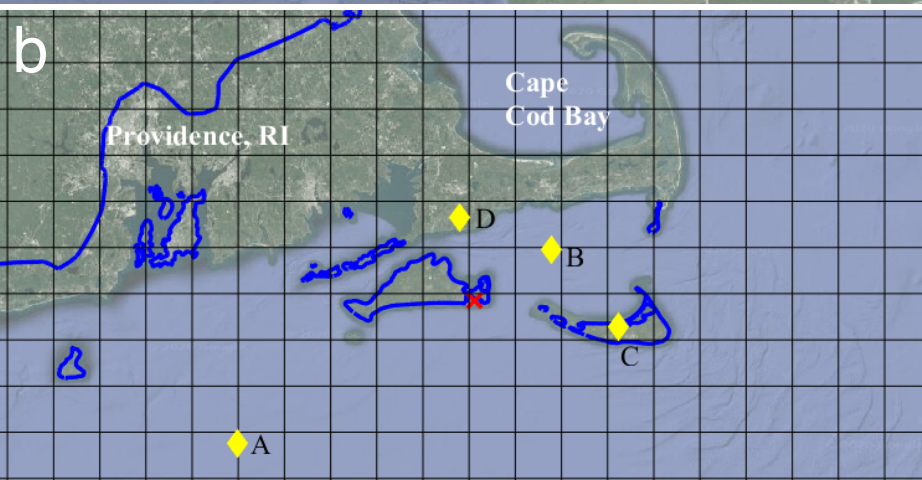
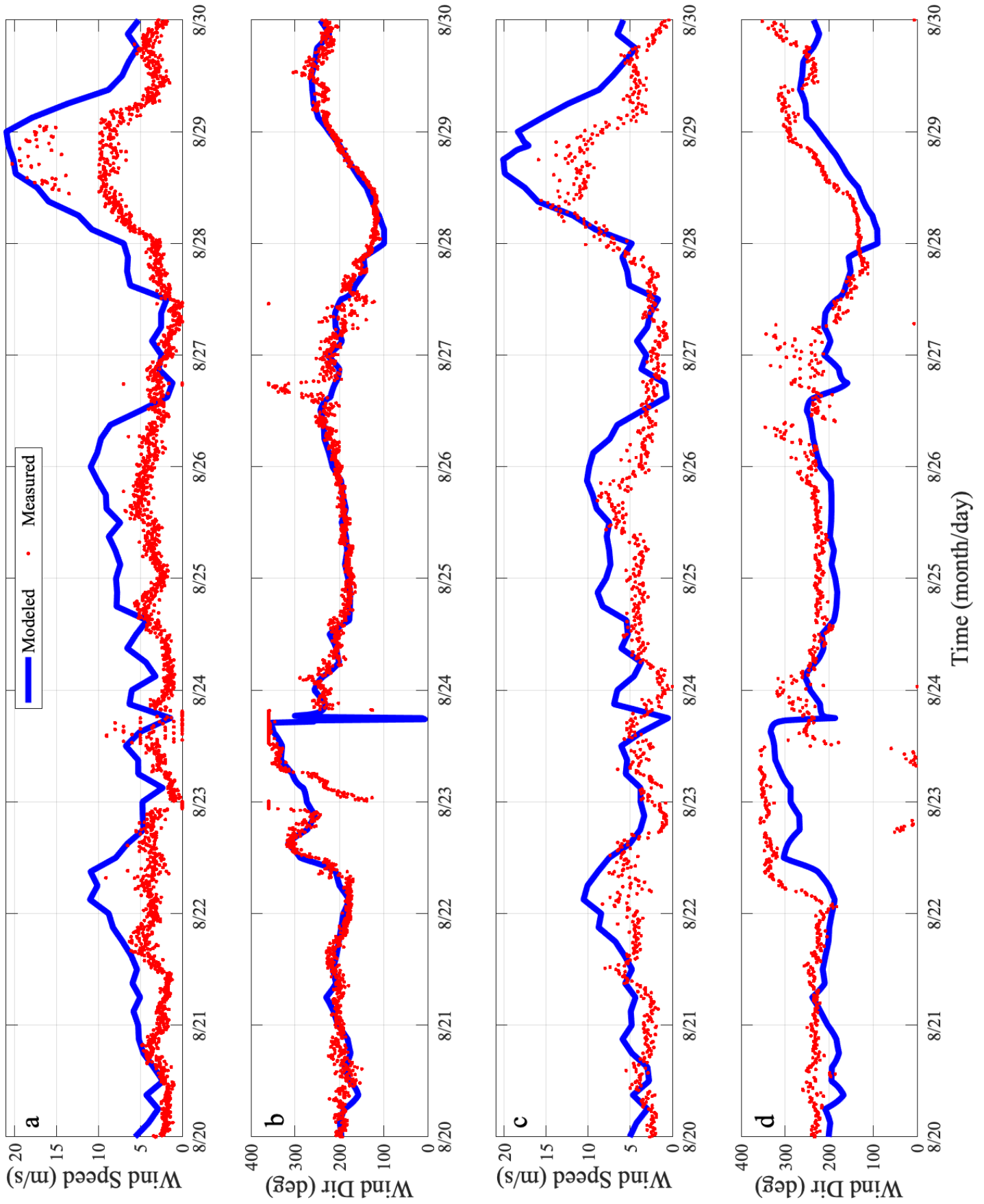
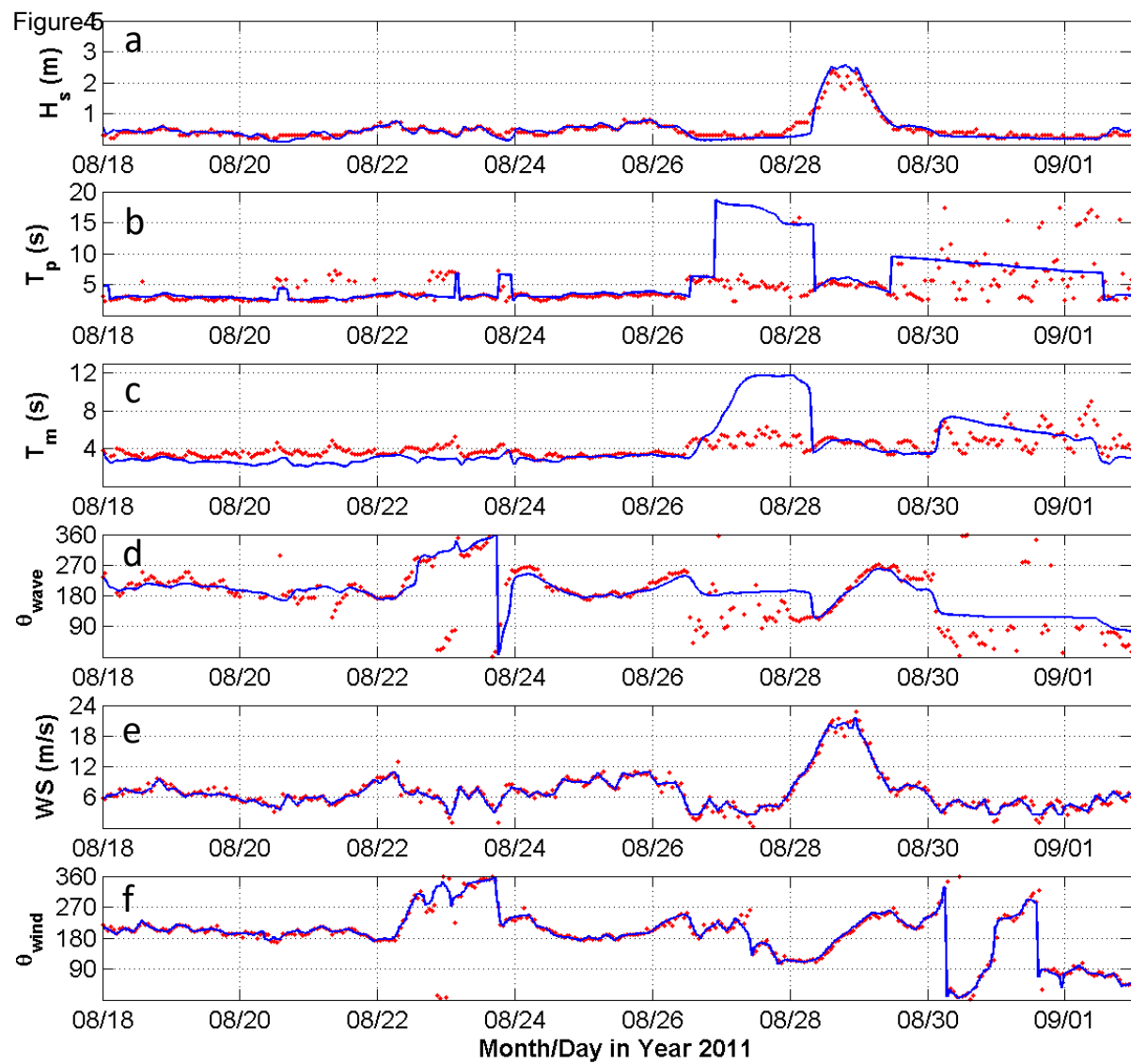


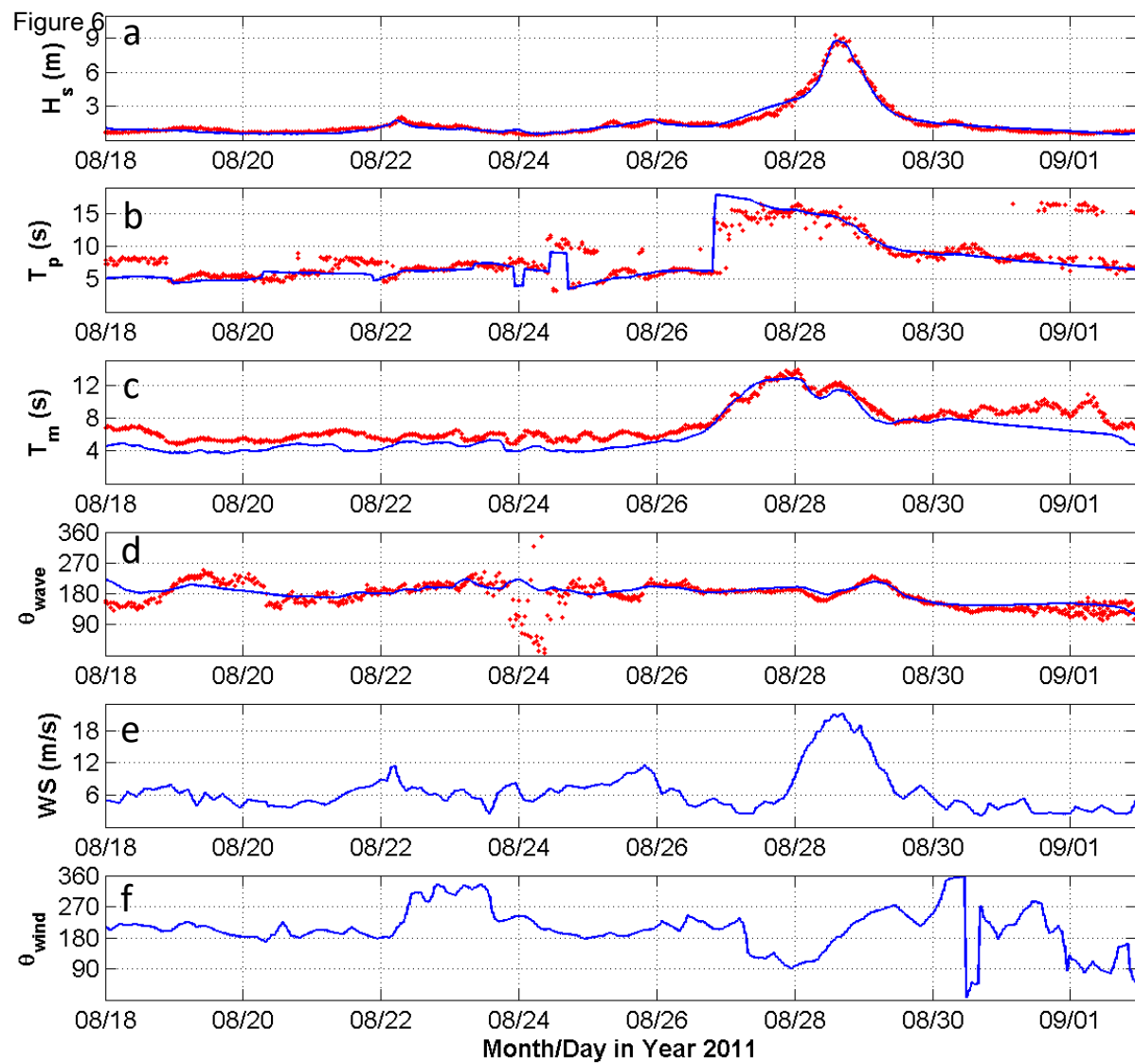
Figure 4

[Click here to access/download;Figure;Figure4\\_subplot\\_nantucket\\_island\\_and](#)









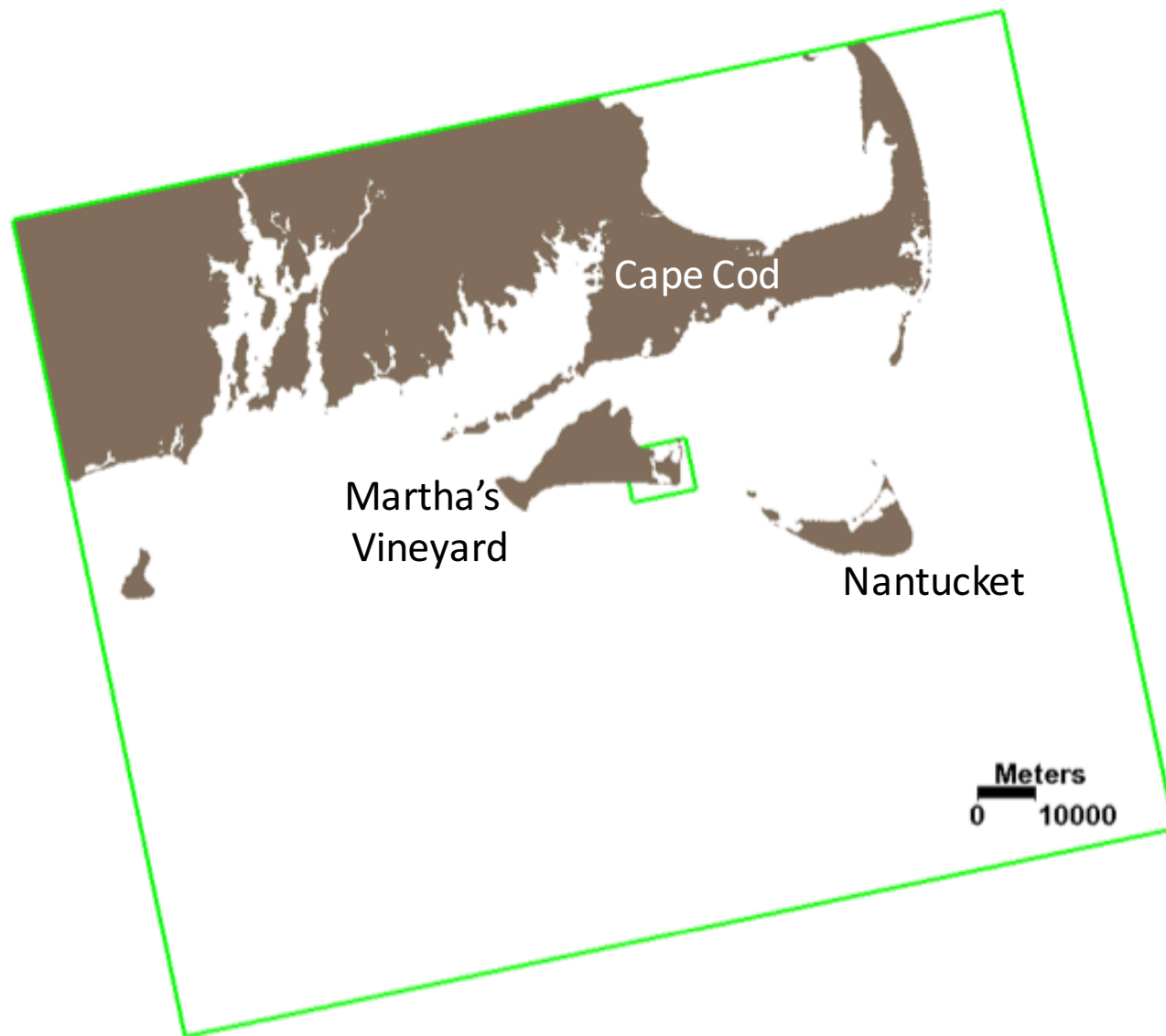
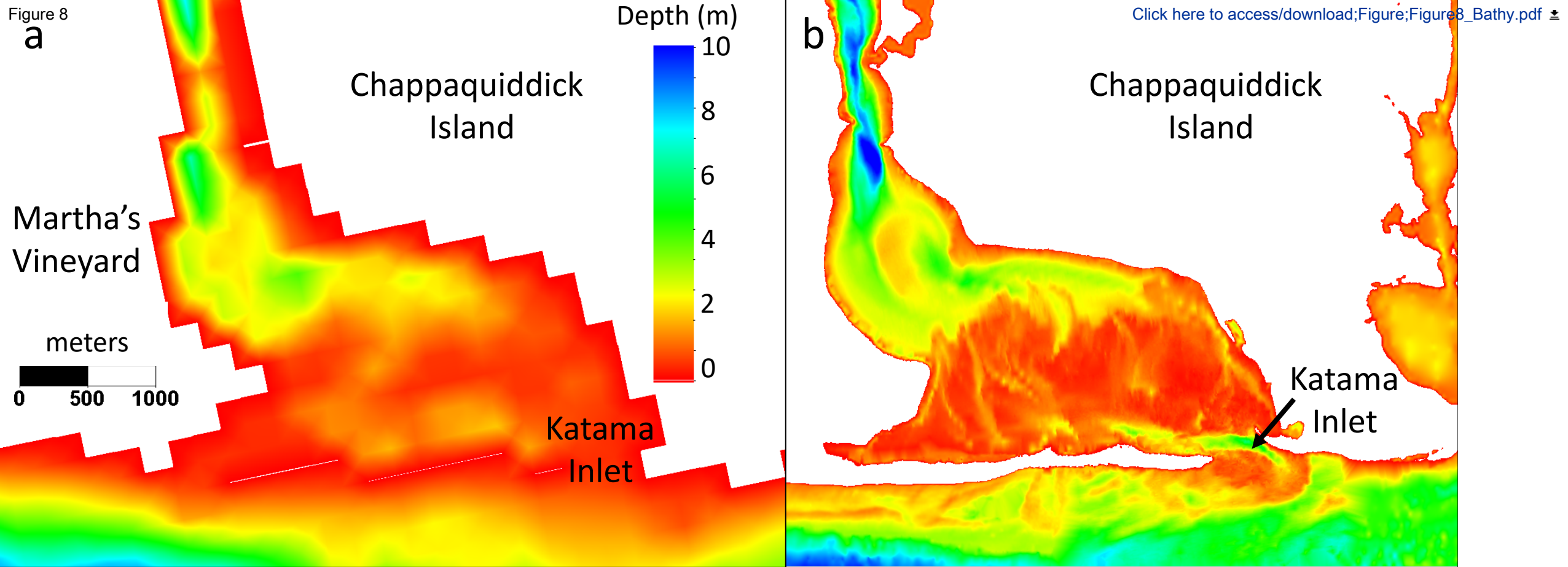
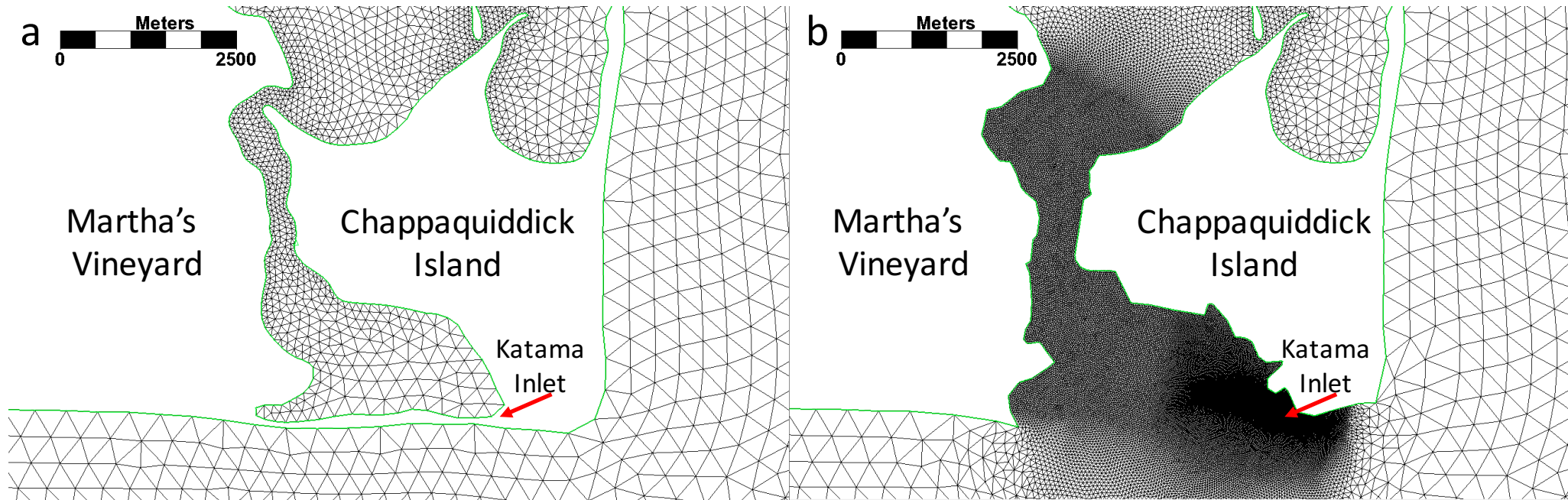


Figure 8





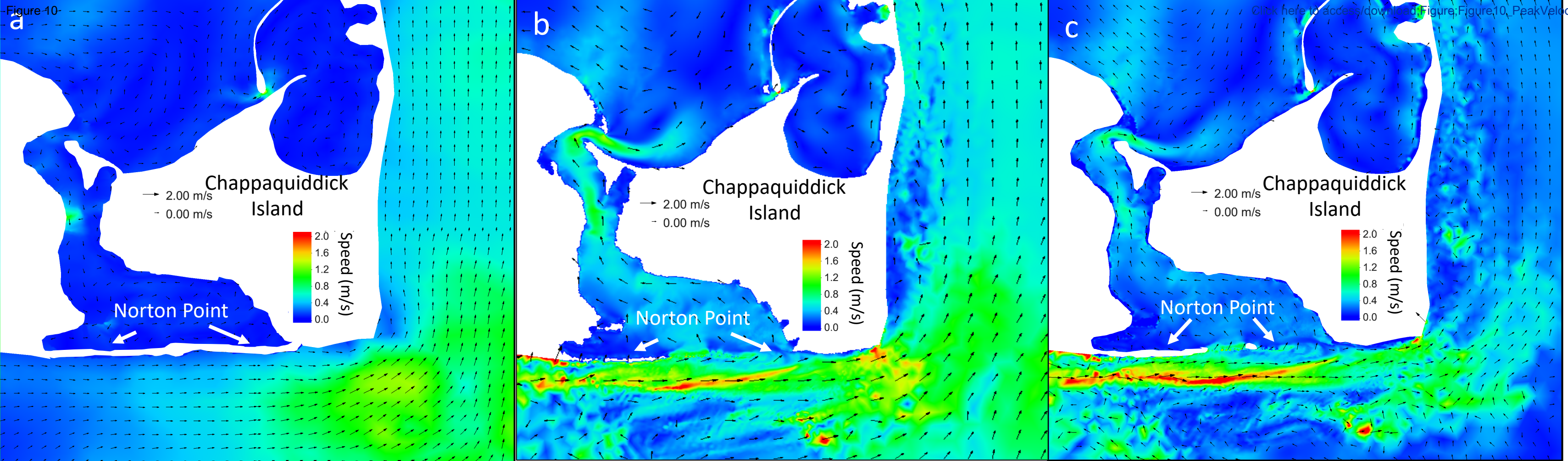
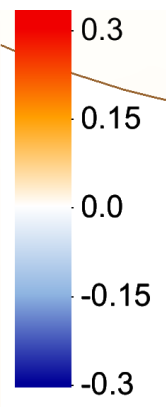


Figure 11  
Elevation Difference (m)

[Click here to access/download;Figure;Figure11\\_Surge\\_073019.pdf](#)



Martha's  
Vineyard

Chappaquiddick Island

Katama  
Inlet

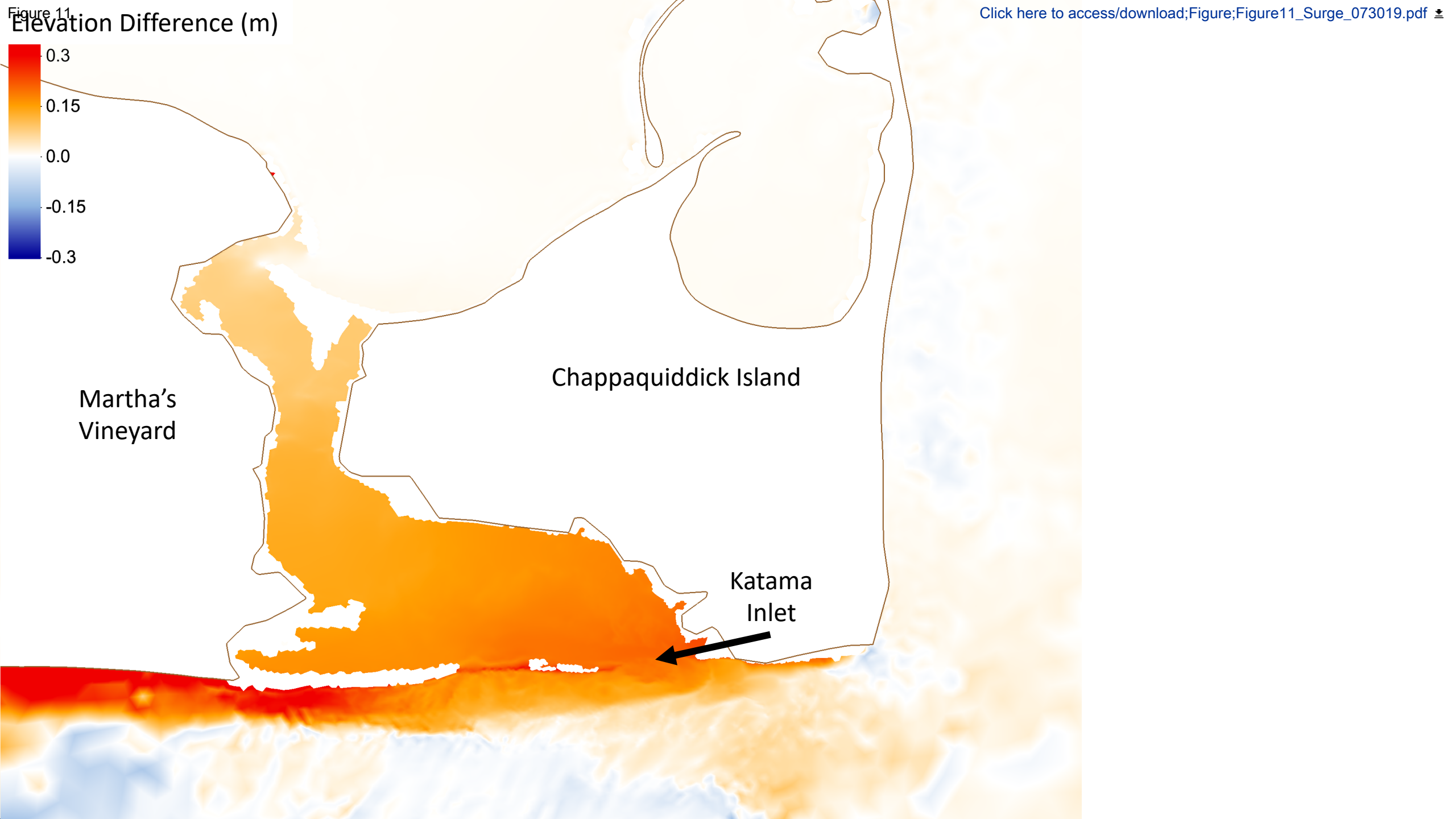
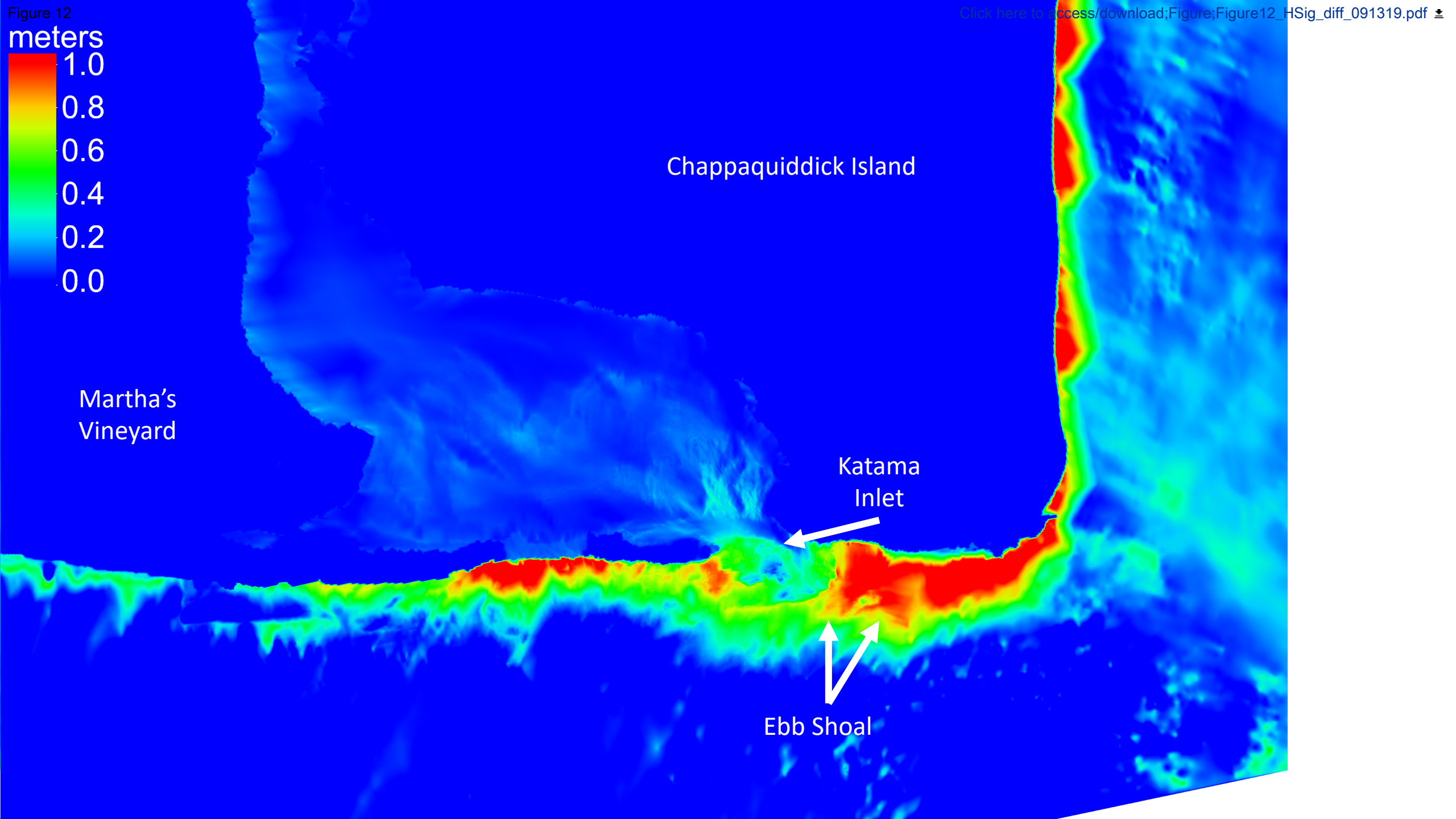
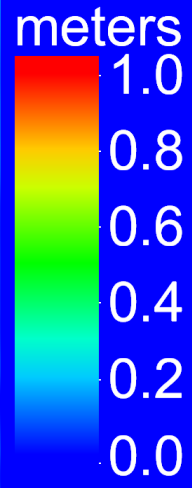


Figure 12





May 25, 2020

To the Editor,

We thank the reviewers and editor for their helpful comments regarding our manuscript “Modeling Storm Surge in a Small Tidal Two-Inlet System”. We have addressed all comments in the text. The largest change was in adding a description of the driving wind and wave models, resulting in new figures and an additional co-author, Robert E. Jensen. We believe the revised manuscript is improved and more thorough, in large part owing to the referees’ suggestions.

Please provide us with any additional feedback. We look forward to hearing from you.

Sincerely,  
Mara M. Orescanin

.....  
Detailed comments on our revision:

***Comments from Reviewer #1:***

*I would like to see how well the winds are represented in the domain. The figure below, which is a screenshot of the NDBC webpage, shows significant number of assets in the region that measured wind speed and direction. Any number of those stations could be used to document the accuracy of the wind field.*

We added a section detailing wind inputs and included several new figures showing observed and modeled wind speed and direction (Figures 4,5, and 6). We agree this helps strengthen the modeling description.

*In the above figure, there are also 3 NDBC buoys (44097, 44090, 44020) of which at least the latter two can be used to verify the accuracy of the wave model. This is especially critical considering the conclusion that coupling waves with circulation is important –which I agree with, as long as the waves are predicted correctly. Also, since Irene was such a large storm and travelled all the way up the Atlantic coast, there is the potential that significant energy in the swell may not have been captured by the domain size restriction of STWAVE.*

The new figures 5 and 6 show model-data comparisons of wave height, period, and direction, and wind speed and direction at two of the NOAA buoys.

*I do not expect the low resolution model to show significant coastal currents (Figure 6). A better comparison would be between the stand-alone high resolution ADCIRC result and the coupled system at the same resolution. This would also reveal the extent of the wave driven currents.*

Good suggestion. Figure 10 (used to be Figure 6) now also shows the currents for the high-resolution no wave model (KB-ADCIRC). This emphasizes the relative importance of wave forcing to the coastal enhanced current.

*Error reduction values of 16% for the uncoupled ADCIRC and 30% for the coupled system are based on a 12 hr window centered at the peak of the storm surge, based on the average of the three locations in the inlet. What would the values be if the time window was expanded to 24 hrs and 36 hrs?*

We prefer to retain the error calculation at 12 hours because it encompasses the peak surge. That is when waves become most important, and thus is of most interest here. As the length of the averaging window increases, the reduction in error approaches the error of the full time series.

*Looking at the observations in figure 2, it seems that the effect of the storm starts around the later part of Aug 27th with a moderate wind event that dies down just prior to that. There is a gradual increase in water level at station 01 and 02 starting between the 25th and 26th which is sustained all the way through the storm. Changing the time scale of the plot window (and analysis time) to start on or around the 25th would provide a better measure of how well the modeling system performs during the high wind event.*

We agree that starting Fig 2 on Aug 25 would focus the figure on the storm. However, we think it is important to display and discuss the pre-storm performance of the models, as well as their performance during the storm, as well as to place the high waves and strong winds during the passage of Hurricane Irene into perspective.

***Comments from Reviewer #2:*** ADCIRC 2-D model will be significantly impact by the bottom roughness, and wonder if this is the reason for the simulation to be very sensitive to the bathymetry? In addition, can author elaborate a little bit towards the wave-current coupling. Overall, a nice job but I also suggest authors to review work from other study sites. For examples:

We agree that bottom roughness is important, and thus instead of a universal roughness (via a single Manning's n) we used a spatially varying roughness near and inside the bay that was determined in a previous study (Orescanin et al. 2016) to provide the best model results compared with observations.

We have added more detail about the coupling of currents and waves.

*Kang, X., & Xia. M. (2020). The Study of the Hurricane-Induced Storm Surge and Bay-Ocean Exchange Using a Nesting Model. Estuaries and Coasts, DOI: 10.1007/s12237-020-00695-3*

Mao, M., & Xia, M. (2018). Wave-current dynamics and interactions near the two inlets of a shallow lagoon-inlet-coastal ocean system under hurricane conditions. *Ocean Modelling*, 129, 124-144. doi: <https://doi.org/10.1016/j.ocemod.2018.08.002>

Mao, M., & Xia, M. (2016). Dynamics of wave-current-surge interactions in Lake Michigan: a model comparison. *Ocean Modelling*, 110, 1-20.  
doi: <http://dx.doi.org/10.1016/j.ocemod.2016.12.007>

As suggested, in the Introduction we have cited 2 of these papers (thank you) that use different models.

**Comments from Reviewer #3:** First I will point out, to the authors and the editors, that I have reviewed a previous version of this paper that was submitted to different journal. Overall, I find that this submission is an improvement and hence my review is short.

I am not sure if this paper was submitted as a "research article", but it is short and I feel it is more like a "technical note". However, the application of these wave (STWAVE) and hydrodynamic (ADCIRC) models in different coupled and uncoupled modes to simulate flow in an ocean/inlet/bay/channel system yields interesting and important results. The paper covers the very interesting and difficult problem of resolving a small and dynamic system that is impacted during a strong storm event. Water level data from 3 pressure sensors deployed over a relatively small area are used to validate the model and understand the hydrodynamics during Hurricane Irene.

The paper lacks a description of all the model parameters. The wave model bathymetry and grid are described (L134-156), but the frequency resolution and other standard parameters are missing. Similarly for ADCIRC, the information needed for one to reproduce the model setup is missing. For example, L188-190 oddly lists parameter names but not the values. Adding the numbers here is an easy addition to the paper and is highly important. Alternatively, the values could be provided in a table.

We have included all specifics of model details including values (or references to figures where model parameters are shown).

More attention could also be given to revising the sentence structure, in making sure that each sentence conveys meaning. As examples, the section on 'Resolution Effects' is very confusing with L244 ("at least up to an upper convergence point") and very long sentences from L244-249 and from L250-255.

Overall I recommend minor revisions to give the authors the opportunity to add more detail about the model setup and improve the writing.

We agree that some of our original sentences were long or confusing, and we have revised the offensive text as suggested.